DISSIPATIVE SYSTEMS AND THEIR CHAOTIC ATTRACTORS

by

Kumela Tafa

A thesis submitted in (part) fulfilment for the degree of Master of Science in Physics in the Addis Ababa University.

June 1990

Addis Ababa

ACKNOWLEDGEMENTS

I would like to express my appreciation and gratitude to all my Instructors from whom I learnt much and for their help during my stay here at the School of Graduate Studies. Above all, my deepest gratitude and special thanks are due to my Instructor and Advisor Dr. J. Jelen who continuously supervised and guided my work.

I continue to be indebted to all friends and people who helped me in preparing the manuscript.

I am also indebted to Ato Girma Dagne who did an excellent job in preparing the technical part of the thesis.

The facilities given me by the Physics Department of AAU and the financial support of the Ministry of Health are greatly appreciated.

K.T.

June, 1990

CONTENTS

		page
INTRODUCTION		1
CHAPTER 1	DYNAMICAL SYSTEMS	4
1.1	General Catagories of Dynamical Systems	4
1.2	Identification and Characterization of a Dynamical Regime	7
1.2.1	The Fourier Transform	9
A	Discrete Fourier Transform	9
B	Different Kind of Fourier Spectra	12
1.2.2	Poincare Sections	17
A	Construction and Properties	17
B	Different Kinds of Poincare Sections	18
1.3	The Description of Time Evolution-Dynamical Systems	23
1.3.1	One Dimensional Non Invertible Maps	23
1.3.2	Two Dimensional Invertible Maps	32
1.3.3	Systems of First Order Differential Equations and Partial Differential Equations	35
CHAPTER 2	EXAMPLES OF DYNAMICAL SYSTEMS	43
2.0	Introduction	43
2.1	The Compass	43
2.1.1	Descreption	43
2.1.2	Evolution Equations	45
2.2	Lorenz's Treatment of Rayleigh Benard Convection	46
2.2.1	Description	46
2.2.2	Evolution Equations	47

		page
2.3	The Beleusov Zhabotinsky Reaction	51
2.3.1	Description	51
2.3.2	Evolution Equations	52
CHAPTER 3	DIFFERENT TYPES OF ATTRACTORS	54
3.1	Asymptotic Behavior of Dissipative Systems and the Simplest Attractors	54
3.2	Limit Cycles, Simple Periodic Attractors .	58
3.3	Bifurcating Periodic Attractors	58
3.4	Strange (Chaotic) Attractors	60
3.4.0	Introduction	60
3.4.1	Characterization of Chaotic Regime	62
3.4.2	Properties of Chaotic Attractors	64
3.4.3	Chaotic Attractors in Nature	68
CHAPTER 4	CHARACTERIZATION OF CHAOTIC ATTRACTORS	73
4.0	A Synopsis	73
4.1	Fractal Dimension	74
4.2	Characterization of Chaotic Attractors . .	76
4.2.1	Dimensions of Chaotic Attractors	76
4.2.2	The Lyapunov Exponent and Kolmogroff Entropy	83
4.3	Characterization of an Attractor by a Measured Signal	91
4.4	Experimental Illustrations of Chaotic Attractors	99
CONCLUSION	. . . . .	107
REFERENCES	. . . . .	108

ABSTRACT

In this work recent developments in the study of non-linear dynamics as applied to dissipative systems, those which exhibit erratic (or chaotic) behavior, are reviewed. As these systems possess chaotic attractors much emphasis is placed on characterization of these sets. In particular the reconstruction of an attractor from a measured signal (single variable) is stressed. Experimental illustration as to how the methods of non-linear dynamics are applied in characterization of chaotic attractors are briefly reviewed from different fields.

INTRODUCTION

According to the previous customs science is called upon to search for simple relations and dependences in the involved and tangled picture of the surrounding world. In addition, perhaps, the natural striving for beauty and order, have long been responsible for the fact that physics has focused all its attention on relatively simple processes (motions). It seems that precisely these processes are realised in overwhelming majority of practically and fundamentally important systems and only in truly complex' systems to resort to statistical description. This thinking, as mentioned, was a result of the ideology of linear physics - the superposition principle admitted no interaction of perturbations, which were responsbile for their stochastization.

Hence linear physics failed to describe truly complex systems such as turbulence, one of the unsolved problems of classical physics. However, recent developments in non linear dynamics have greatly increased our understanding of such problems, and given us new concepts and models of thought that have far reaching repercussions in many different fields (solid state physics, hydrodynamics, plasma physics, chemistry, biology, etc.).

In spite of the fact that it is very hard to answer, what is turbulence, we understand turbuent motion as a motion with a large number of macroscopic degrees of freedom.

Today, however, we know examples of highly complicatred and seemingly chaotic motions which occur with a small number of macroscopic degrees of freedom. This type of motion is described, for instance, by a well-known

Lorenz system of three ordinary nonlinear differential equations. This model led to the discovery of a 'chaotic attractor', which is a restricted region in phase space (3-D phase space in case of the Lorenz system) that attracts all trajectories from the neighborhood. Such a phenomenon is a typical property of 'dissipative dynamical systems'.

The realization that finite dimensional dissipative systems can have chaotic attractors on which the motion is everywhere unstable has brought a new perspective to non-linear dynamics. Motion on the attractor depends sensitively on initial conditions (near by points diverge at an exponential rate on the average) and the sensitive behavior leads to an apparently stochastic time signal with a broad band power spectrum. The finite amount of information contained in finite accuracy specification of the initial state is eroded by the flow and once sufficient time has elapsed to uncover the unknown part of the initial data, the state of the dynamical system is unpredictable. Although Poincare and few others were fully aware that Hamiltonian systems could exhibit such behavior, it was not widely appreciated until the early seventies, following the Poineering work of Lorenz in weather prediction models and the bold and imaginative ideas of Ruelle and Takens that dissipative systems could have unstable asymptotic behavior. This long time sensitivity behavior of a finite order system of ordinary diferential or difference equations is reffered to as chaos.

As the asymptotic behavior of dissipative systems can be well described by studying their attractors, much emphasis is given to the study of attractors in particular to characterization of chaotic attractors. Such a topic - chaotic attractors - has found abundant applications in a wide variety of

physical situations. The list of these applications include, problems in the onset of turbulence in fluids, chemically reacting systems, nonlinear wave interaction in plasma, solid state physics, etc.

The thesis as a whole can be seen as consisting of two parts. The first, which constitutes two chapters is introduction to dynamical systems, where we see some methods of characterization of dynamical regimes followed by examples of dynamical systems. The second part, which again consists two chapters is devoted to the study of attractors, where we start with the simplest attractors and went on to characterization of chaotic attractors. Here reconstruction of a chaotic attractor from a measured signal is stressed. And finally, experimental illustrations of chaotic attractors from different fields are briefly reviewed. It is hoped that the study of chaotic attractors will shed much light on the understanding of truly complex systems from different branches of science.

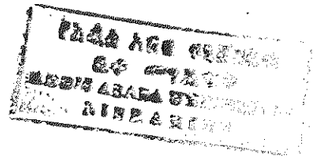

CHAPTER 1

DYNAMICAL SYSTEMS

1.1 General Catagories of Dynamical Systems

Let M be a differentiable manifold a differentiable map $\psi : \mathbb{R} \times M \to M$ is said to be a dynamical system[1] or a flow on M if for all $x \in M$ and $t,s \in \mathbb{R}$ we have

i) $\psi(0,x) = x$ (1.1a)

ii) $\psi(t, \psi(s,x)) = \psi(t+s,x)$ (1.1b)

This being the definition from mathematical point of view, physicists define dynamical system as any set of equations giving the time evolution of the state of a system from a knowledge of its past history[2]. Examples are, Maxwell's equations, the Navier Stokes equations, and Newtons equations of motion for a particle with specified forces. The Kepler problem and the harmonic oscillator falls under the last example. We know that these two are solvable problems. As another example consider a damped pendulum, whose equation of motion is given by:

$$\ddot{\theta} + 2\gamma\dot{\theta} + \omega^2\theta = 0 \qquad (1.2)$$

where $\dot{\theta} = \frac{d\theta}{dt}$, γ the damping coefficient and ω the frequency

Fig.1.1 Simple pendulum with damping

The general solution to this equation is given by

$\theta(t) = \theta(0)e^{\alpha t}$, where α satisfies the characteristic equation

$$\alpha^2 + 2\gamma\alpha + \omega^2 = 0$$

or $$\alpha_{1,2} = -\gamma \pm \sqrt{\gamma^2 - \omega^2} \qquad (1.3)$$

Hence we see that, in the limit $t \to \infty$ (for $\gamma > 0$) the pendulum will be at the equilibrium position due to the factor $e^{-\gamma t}$. This equilibrium

position to which all trajectories converge (in phase space) for $t \to \infty$ is said to be a fixed point attractor.

Quite soon one learns that not all dynamical problems are explicitely solvable even alowing for solutions interms of the more complicated transcedental functions. This situations may occur for systems with few degrees of freedom (i.e. few dynamical variables), and without external noise[3] . Furhter more, it is not restricted to Hamiltonian systems, but appears as well for dynamical systems with internal friction called dissipative (or non conservative) dynamical systems, to which we limit ourselves in this work. The reason for this difficulty is the fact that dynamical problems with regular equations may have solutions which behave irregularly in time.

The interest in studying non-linear systems is to understand, in the absence of explicit solutions, more about the qualitative aspects of these irregular solutions. There is no gneral classification of dynamical systems which is sufficiently enough to account for all possible types of erratic behavior of their solutions and even such simple systems as forced pendulum with friction are exceedingly hard to analyze.

Even though this classification is far from the analysis of erratic behavior of dynamical systems we put them into two catagories as whether the flow contracts volume in phase space or not. Our interest is in the former ones and these systems are referred to as dissipative systems. Those systems for which the flow will not contract volume in phase space are called Hamiltonian or conservative systems.

What is the criteria for contraction of volume in pahse space, which guarantees that the systems under discussion are dissipative?

The evolution of numerous systems is described by a set of n first order ordinary differential equation:

$$\frac{d}{dt}\underline{x} = \underline{F}(\underline{x}) \tag{1.4}$$

where $\underline{x} \in \mathbb{R}^n$ (the phase space) and $\underline{F}$ is a vector field over this space. For contraction of volume in $\mathbb{R}^n$ in such a case

$$\frac{dv}{dt} < 0 \tag{1.5}$$

For $v > 0$ this can be written as $\frac{1}{v}\frac{dv}{dt} < 0$. But by the Lie derivative we do have

$$\frac{1}{v}\frac{dv}{dt} = \sum_{i=1}^{n} \frac{\partial \dot{x}_i}{\partial x_i} \tag{1.6}$$

where $\dot{x} = \frac{dx}{dt}$. Therefore, $\underline{F}$ contracts volume in $\mathbb{R}^n$ when

$$\sum_{i=1}^{n} \frac{\partial \dot{x}_i}{\partial x_i} < 0 \tag{1.7}$$

In case of dynamical systems that are described by difference equation of the form:

$$\underline{x}_{n+1} = \underline{f}(\underline{x}n) \tag{1.8}$$

the Jacobian matrix J of the map plays the role of the Lie derivative. When this is the case, the criteria reads:

$$\det J < 1 \tag{1.9}$$

where $J_{ij} = \frac{\partial f(x_i)}{\partial x_j}$

From the above analysis, it is seen that for a damped pendulum the origin is an attractor. Now let us modify the equation of motion of that pendulum such that

$$\gamma = \gamma(\theta) - \theta^2 \tag{1.10}$$

For instance suppose $2\gamma = -(\varepsilon - \theta^2)$ in equation (1.2). Given that $\varepsilon > 0$ the trajectories diverge as spirals in the neighborhood of the origin. In fact in this region θ is always small and the term in θ^2 remains negligible. Then we find ourselves in the situation depicted in Fig.1.2a.

By constrast, far from the origin the trajectories tend to this singular point, since $\gamma(\theta)$ is then positive. Intutively, we can hypothesize that there exists a closed trajectory between these two extremes encircling the origin.

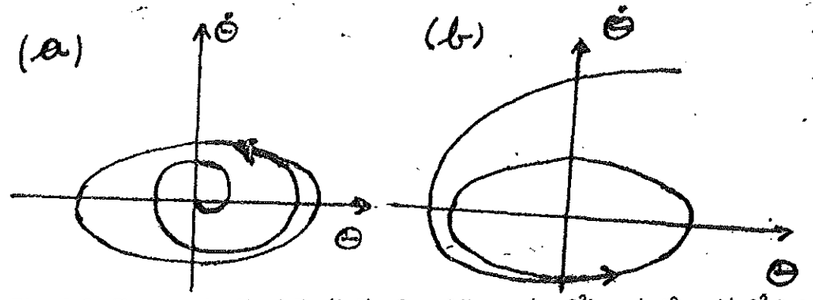

Fig. 1.2 Phase protrait of Eq.(1.2) for $2\gamma = -(\varepsilon - \theta^2)$ a) $\theta^2 < \varepsilon$ b) $\theta^2 > \varepsilon$

So, the attractor is now another regime of phase space. Fig.1.2 (a and b) clearly indicate this. The spirals near the origin as well as those far away from the origin tend to a single closed integral curve of Fig.1.2, which in its turn corresponds to a periodic solution of Eq.(1.2). Occurences of this kind were first studied by poincare, who gave the name limit cycle (or simply cycle) to a closed solution curve of the kind we have found in the present case.

1.2 Identification and Characterization of a Dynamical Regime

When, as an outcome of an experiment or numerical simultation, we have a time dependent signal $x(t)$ - called a time series, one of the essential tasks is to determine the kind of evolution that produced it. Here our intention is to compress information in such a way that the most significant dynamical characteristics are emphasized. In ohter words, what is it that we are dealing with? Is it an oscillation more or less complicated in shape, but with a perfectly well defined period? Are we dealing with more or less a linear superposition of several different oscillation? Or is it something else entirely?

Except in very simple situation such as Eq.(1.2) with $\gamma = \gamma(\theta)$, where we

can safely say that there exists a periodic solution to the equation of motion, the answer to these questions is not at all trivial.

A description of these solutions includes a period (or equivalently, the frequency) and an amplitude: essentially, the amplitude of the limit cycle, and the time taken to traverse it. These two characterstics will emerge as soon as the equations of motion are known. We underline that these characterstics remain, and play just as essential a role, for periodic phenomenon whose underlying mechanism is unknown, or described by equations that are not soluble analytically, by far the most frequent situation in practice.

Certain dynamical regimes are a superposition of oscillations which differ in amplitude, period ratio of harmonics, etc.[5] As an illustration to what has been said consider the special case of Hill's equation.

$$\ddot{\theta} + \frac{g(t)}{\ell}\,\theta = 0 \qquad (1.11)$$

where g(t) is a time dependent gravitational field. For this particular case

$$g(t) = g_0 + g_1 \cos 2\omega t \qquad (1.12)$$

Eq.(1.11) with g(t) as given in (1.12) is called Mathieu equation. Now let $h = g_1/g_0$ and $\omega_0^2 = g_0/\ell$ then Mathieu equation reads

$$\ddot{\theta} + \omega_0^2 [1 + h \cos (2\omega t)]\,\theta = 0 \qquad (1.13)$$

Let $\alpha = h \cos (2\omega t)$ substitution into (1.11) the two equations we get are:

$$\ddot{\theta} + \omega_0^2 [1 + \alpha]\,\theta = 0 \qquad (1.14a)$$

$$\ddot{\alpha} + 4\omega^2 \alpha = 0 \qquad (1.14b)$$

which describes the behavior of two oscillators of amplitude θ and α. They are coupled by the term $\omega_0^2\,\alpha\,\theta$. The associated attractor is no more a limit cycle, but a torus. This type of regime is said to be 'quasiperiodic', while that whose attractor a limit cycle is called 'periodic'

Other regimes are of a nature more difficult to grasp. Given their completely disordered appearance, we call them "chaotic". As an illustrative example consider the following flow, put forth by Rossler:

$$\begin{aligned} \dot{x} &= -y - z \\ \dot{y} &= x + ay \\ \dot{z} &= b + z(x-c) \end{aligned} \qquad (1.15)$$

where x, y and z are variables, a, b and c parameters to be chosen. For certain values of a, b and c (for instance: a = b = 0.2, c = 5.7), solutions to equations (1.15) exhibit aperiodic or chaotic behavior. When the dynamics is deterministic (i.e. representable by a finite number of nonlinear coupled differential equation or the equivalent), the trajectories in phase space converge onto a 'chaotic attractor', whose topological properties are radically different from those of a torus.

To answer the questions asked at the begining of this section, one must use "objective" method of analysis, not merely the observer's judgement of the regularity of the time series.

There are several ways to identify and to characterize a dynamical regime. Here two frequently used methods will be reviewed very quickly: first, the Fourier transform and then the Poincore sections.

1.2.1 The Fourier Transform

A. Discrete Fourier Transform

The rapid development of computational methods has meant that a signal x(t) - a continuous function of time - is very often measured by sampling and discretizing. Therefore, an experiment generally provides a discrete sequence of real numbers $x_u (u \in Z)$ regularly spaced at time interval of Δt. (See Fig.1.3).

In practice this sequence of numbers should be finite. Practical consideration such as acceptable duration of the experiment, and the capacity

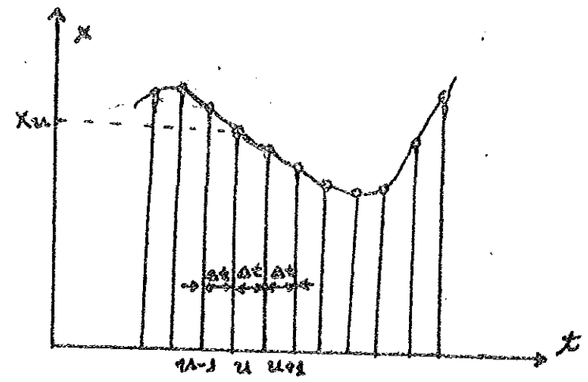

Fig. 1.3 Discretization of a continuous function. The continuous function - for example, an experimental signal is represented by the solid line. The discreti values x_u are taken at the instants....u-1, u, u+1 ... equally spaced at time intervals of Δt . Hereafter, the continuous function is replaced by the series of points P_u. [From reference 5].

for storage and processing of the measurements determines the choice of r and Δt, where r is such that $t_{max} = r \Delta t$

Definition: The function g(s) defined for real s by

$$Tf = \lim_{a\to\infty} \frac{1}{\sqrt{2\pi}} \int_{-a}^{a} e^{-ixs} f(x)dx = g(s) \qquad (1.16a)$$

is said to be the Fourier transform of f(x); the operator T is called the Fourier transform operator.

$$T^{-1}g = \lim_{a\to\infty} \frac{1}{\sqrt{2\pi}} \int_{-a}^{a} e^{ixs} g(s)ds = f(x) \qquad (1.16b).$$

The analog of this definition in the discrete case is

$$\hat{x}_k = \frac{1}{\sqrt{m}} \sum_{u=1}^{m} x_u e^{-i \frac{2\pi uk}{m}} \qquad (1.17)$$

where k = 1, ..., m

The autocorrelation function of the signal x_u is defined by

$$\psi_\alpha = \frac{1}{m} \sum_{u=1}^{m} x_u \, x_{u+\alpha} \qquad (1.18)$$

where

$$x_u = T^{-1} \hat{x}_k = \frac{1}{\sqrt{m}} \sum_{k=1}^{m} e^{i \frac{2\pi uk}{m}} \hat{x}_k \quad \text{and the unit of time}$$

is still Δt so that $\psi_\alpha = \psi(\alpha \cdot \Delta t)$

Physically, this function represents the average of the product of the signal values at a given time and at time $\alpha \cdot \Delta t$ later. One can therefore deduce from ψ_α whether, and for how long, the instantaneous value of the signal depends on its previous values, hence its name. Or else we can say that it is a measure of the degree of resemblance of the signal with itself as time passes.

For x_u periodic in m, the autocorrelation function necessarily has the same property:

$$\psi_\alpha = \psi_{\alpha+m}$$

By applying the inverse Fourier transform, we get:

$$\psi_\alpha = \frac{1}{m^2} \sum_{u=1}^{m} \sum_{k,k'=1}^{m} \hat{x}_k \, \hat{x}_{k'} \, \exp\left[\frac{i2\pi}{m}(uk + (u+\alpha)k')\right]$$

using the property $\hat{x}^*_{k'} = \hat{x}_{m-k'}$ and summing over u and k' we reach at

$$\psi_\alpha = \frac{1}{m} \sum_{k=1}^{m} |\hat{x}_k|^2 \cos(2\pi\alpha k/m) \qquad (1.19)$$

This shows that, up to a factor of proportionality, the autocorrelation function is merely the Fourier transform of $|\hat{x}_k|^2$.

By defining a function S_k such that

$$S_k = \sum_{\alpha=1}^{m} \psi_\alpha \cos\left(\frac{2\pi\alpha k}{m}\right) \qquad (1.20)$$

and substituting this into (1.19) and doing a little bit of manipulation,

one can arrive at,

$$S_k = |\hat{x}_k|^2 = \sum_{\alpha=1}^{m} \psi_\alpha \cos(2\pi\alpha k/m) \qquad (1.21)$$

Which is the sought-after inversion relation (for the derivation of this result see reference 5). This result constitutes one form of the Wiener-KHintchin theorem, which says that the function $|\hat{x}_k|^2$ is proportional to the Fourier transform of the autocorrelation function ψ_α of the signal.

The graph representing $|\hat{x}_k|^2$ as a function of the frequency f($f=k\cdot\Delta f$) is referred to as the "power spectrum".

The power spectrum of a real function has the property

$$|\hat{x}_k|^2 = |\hat{x}_{m-k}|^2 \qquad (1.22)$$

Which comes from the equality $\hat{x}_k = \hat{x}^*_{m-k}$. This expresses the fact that information about the phase of a component $\hat{x}_k$ is lost when we consider $|\hat{x}_k|^2$.

B. Different Kinds of Fourier Spectra

i) Periodic Signal

The appearance of the power spectrum clearly depends on the way in which the signal x(t) evolves over time. The interest of the Fourier spectrum is, in fact, that it reveals properties of the evolution which would otherwise remain undetected.

The spectrum of a periodic signal of period T is made up of a peak at the frequency 1/T, its sidelobes and possibly a certain number of other peaks (and their sidelobes) that are harmonics of the fundamental frequency. This is shown in figure below.

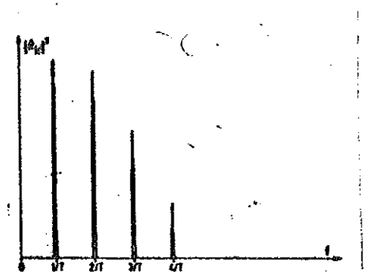

Fig. 1.4 Periodic function containing harmonics. Only the first four harmonics are shown.

ii) Quasiperiodic Signal

A function y of r independent variables is said to be periodic, of period 2π in each of its arguments, when increasing one of these variables by 2π does not change its value:

$$y(t_1, t_2,\ldots,t_r) = y(t_1, t_2,\ldots, t_i + 2\pi,\ldots,t_r) \qquad (1.23)$$

where $i = 1,2,\ldots,r$.

Such a function is said to be quasiperiodic in time if its r variables are all proportional to the time t:

$$t_i = \omega_i t , \quad i = 1,\ldots,r \qquad (1.24)$$

A quasiperiodic function has r fundamental frequencies:

$$f_i = \omega_i/2\pi, \quad i = 1,2,\ldots,r \qquad (1.25)$$

As one might guess, the Fourier spectrum of a function which is quasiperiodic in time generally has relatively complex appearance. In general, the Fourier spectrum of a quasiperiodic function x(t), which depends non linearly on periodic functions of the variables $\omega_i t$, contains components at all frequencies of the form:

$$|m_1 f_1 + m_2 f_2 + m_3 f_3 + \ldots + m_r f_r|$$

where m_i are arbitrary integers.

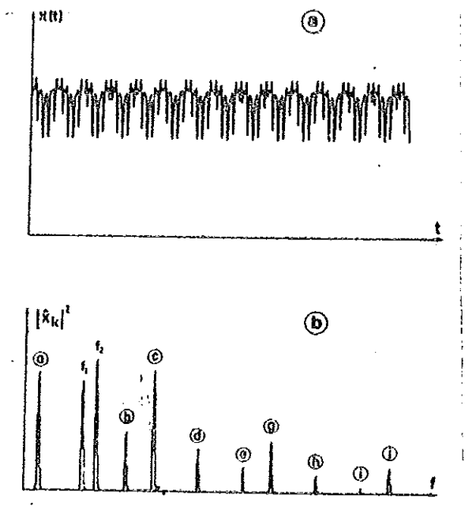

Fig. 1.5 Quasiperiodic function with two frequencies f_1 and f_2 (the ratio f_1/f_2 is irrational)

a) time series

b) Fourier spectrum containing, besides the two fundamental frequencies f_1 and f_2, the principal peaks of frequency $f = m_1 f_1 + m_2 f_2$

a → $f_2 - f_1$	d → $3f_1$	h → $5f_1$
b → $3f_1 - f_2$	e → $5f_1 - f_2$	i → $7f_1 - f_2$
c → $f_1 + f_2$	g → $3f_1 + f_1$	j → $5f_1 - f_2$

(From reference 5).

Under the hypothesis, f_1/f_2 is rational, the Fourier spectrum is not dense. It follows that the spectrum is definitely not represented by a continuous function since:

$$f_1/f_2 = n_1/n_2 \quad (n_1, n_2 \text{ integers}) \tag{1.26}$$

the quasiperiodic signal is in fact periodic with period

$T = n_1T_1 = n_2T_2$. Indeed, according to the definition, one has:

$$x(\omega_1 t, \omega_2 t) = x(\omega_1 t+2\pi n_1, \omega_2 t+2\pi n_2) = x(\omega_1(t+\frac{n_1}{f_1}), \omega_2(t+\frac{n_2}{f_2})) \qquad (1.27)$$

One says that there is frequency locking of f_1 with f_2. All the lines of Fourier spectrum are harmonics of the lowest frequency

$$f_o = 1/T = f_1/n_1 = f_2/n_2$$

The following figure depicts this possibility. Consecutive lines of the spectrum are always separated by the same distnace of 1/T.

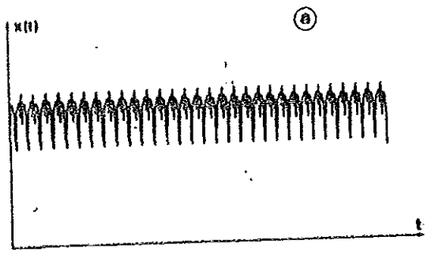

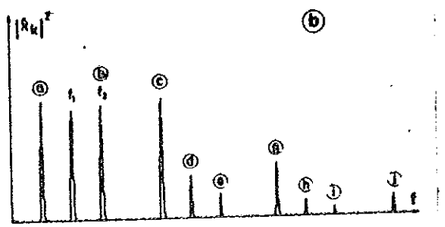

a → f_2-f_1
b → 3f(= f_2)
c → 5f
d → 6f
e → 7f
g → 9f
h → 10f
i → 11f
j → 12f

Fig. 1.6 Quasiperiodic function (f_1/f_2 rational)

a) Time series

b) Fourier spectrum. The function is almost identical to that shown in Fig. 1.5 but f_1 is changed in such a way that $f_1/f_2 = 2/3$. Note that under this condition, all the peaks are harmonics of the frequency $f = f_2-f_1 = 1/3\ f_2$.

iii) Aperiodic Signal

When the signal x(t) is neither periodic nor quasiperiodic, it is called aperiodic (or some times non-periodic). The Fourier spectrum of such a signal is continuous. The real difficulty is that a Fourier spectrum which looks continuous cannot be automatically attributed to an aperiodic signal, because this is also the appearance of the spectrum of a quasiperiodic singal with a very high number of frequencies ($r \to \infty$).

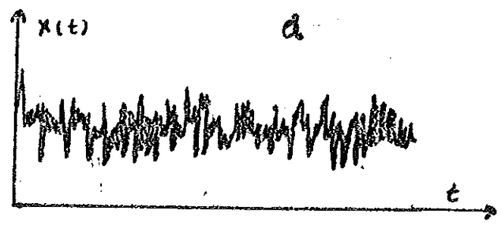

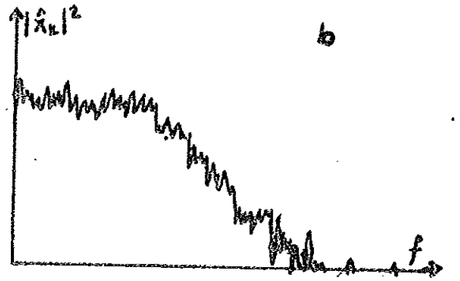

Fig. 1.7 Aperiodic function

a) Time series

b) Fourier spectrum. Note the continuous nature of this spectrum in contrast to the line spectra of Figures (1.5) and (1.6).

Above, we have already indicated that the spectrum of an aperiodic signal has a continuous appearance. Is the signal purely random or aperiodic? In other words, is the signal random so that we apply probabilistic approach for its description or is there some hidden

determinism behind? So this method of analysis does not distinguish between an aperiodic and a random signal. This limits the application of Fourier transform, leading as to the other methods, notably that of poincare sections.

1.2.2 Poincare Sections

A) Construction and Properties

In the remainder of Sec. (1.1) we know that the evolution of numerous systems is described by a set of n first order differential equation of the form $\dot{\underline{x}} = \underline{F}(\underline{x}(t))$.

Rather than directly studying the solution to the above mentioned equation in R^3, it can be fruitful to observe the points of intersection of the trajectory with a plane.

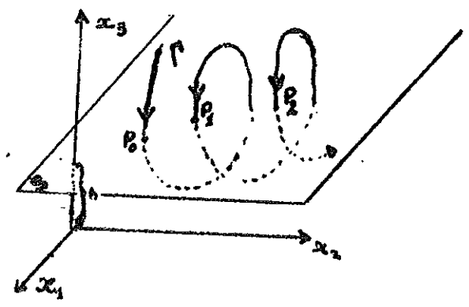

Fig. 1.8 Illustration of a Poincare Section. The phase trajectory Γ intersects the plane S (with $\dot{x}_3 < o$) at successive points P_o, P_1,... . This points belong to the poincare section of M with the plane S.

S can be any plane, but an appropriate choice yields sections that are more easily analyzed. Starting with an initial condition, one thus obtains a set of points comprising the Poincare sections. i.e., a graph in two dimensions.

The transformation leading from one point to the next is a continuous

mapping T of S into itself called Poincare's Map:

$$P_{k+1} = T(P_k) = T(T(P_{k-1})) = \ldots \qquad (1.28)$$

Since the solution to the flow is unique the point P_0 completely determines P_1, which in turn determines P_2, and so on. If inversely, P_1 uniquely determines P_0 by reversing the sign of t in the equation of the flow ($\dot{\underline{x}} = \underline{F}(\underline{x})$), then T is an invertible mapping of S into itself. Therefore one can say that the Poincare section replaces the continuous time evolution of a flow with a discrete-time mapping.

Finally, it should be emphasized that, by construction, the Poincare section and map have the same kind of topological properties as the flow from which they arise.

The method of Poincare sections simplifies the study of continuous flows for three reasons:

a) Reduction of coordinates by one.

b) The time is discretised and differential equations are replaced by difference equations defining the Poincare map $P \to T(P)$.

c) The quantity of data to be manipulated is greatly reduced, since almost all the points on the trajectory can be ignored.

B. Different Kinds of Poincare Sections

i) Periodic Solution

Following the procedure of section 1.2-1 (B) we shall examine the Poincare's section of an attractor according to the dynamical properties of the corresponding solution, when the solution

is periodic the phase trajectroy is a closed orbit, the limit cycle. The corresponding Poincare section is very simple reducing to a single point as shown below, or possibly several points

Fig. 1.9 Poincare Section of a limit cycle.

when the limit cycle has a tortuous form. The point is a fixed point of the Poincare map T since:

$$P_0 = T(P_0) = T^2(p_0) = \ldots \qquad (1.29)$$

ii) Quasiperiodic Solution

For a biperiodic solution with two fundamental frequencies f_1 and f_2, we know that the attractor is a torus T^2 that can be drawn in R^3. Any attractor on the surface of the torus can be seen as the superposition of two motions:

a) Rotation along the larger dimension

b) Rotation about the axis of the "cylinder" forming the torus.

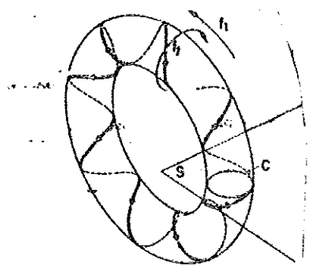

Fig. 1.10 Torus T^2 and its Poincare section. With the plane S.
The two frequencies with which the torus is traversed are designated by f_1 and f_2. Under the assumption f_1/f_2 is irrational, the Poincare section is the closed curve C. (Taken from reference 5).

Each fundamental frequency f_1 and f_2 is associated with one of these rotational motions. The points of intersection of a trajectory with a plane of section S appear at regular time intervals equal to the period of the first motion. (Here, $T_1 = 1/f_1$). The points are located on a closed curve C whose form can be either

-Simple: i.e., with no points of self intersection, (circle, ellipse, etc.).

-More complicated (such as cycloid, etc.) in the presence of harmonics of f_1 and f_2.

The exact form of the Poincore section depends on the ratio f_1/f_2. If it is irrational, the trajectroy never closes on itself and densely covers the surface of the torus. One also says in this case that the two frequencies are incommensurate. The closed curve C is then continuous. Since each of its points is the image under T of another point of C, the curve is invariant under the mapping T:

$$T(C) = C \tag{1.29}$$

The curve C, though itself continuous, is not traversed continuously by successive intersection points of the trajectory with the plane S. On the contrary, the mapping T corresponds to a finite shift along C.

When the ratio f_1/f_2 is rational, the poincore section is composed of a finite set of points distributed along C. However, C is no longer a continuous curve, for the trajectory is not dense on the torus. There is frequency locking between f_1 and f_2: the ratio f_1/f_2 is equal to that of two integers n_1 and n_2. After having n_1 circuits and n_2 "rotations the trajectory closes upon itself;

we are infact dealing with a periodic solution of period $T = n_1/f_1 = n_2/f_2$. The Poincare section contains only n_1 points such that

$$P_i = T^M(P_i) \tag{1.30}$$

In Fig.1.11, the two possibilities are summarized.

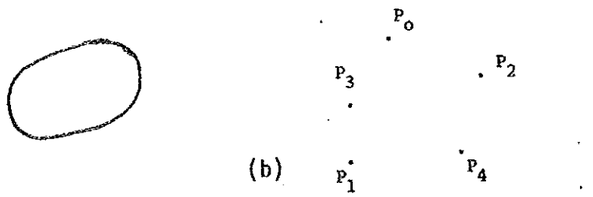

Fig. 1.11 Poincare section for quasiperiodic regime with two frequencies f_1 and f_2.

a) f_1/f_2 is irrational

b) f_1/f_2 is rational, 3/5 in this case. The index specifies the the order in which the points P_0, P_1, P_2, P_3 and P_4 are traversed.

iii) Chaotic Solution

Let us finally, have a look at a simple nonintegrable example from classical mechanics which displays chaotic motion. Its Hamiltonian M is given by[6]

$$H = \frac{1}{2} \sum_{i=1}^{2} (p_i^2 + q_i^2) + q_1^2 q_2 - \frac{1}{3} q_2^3 \tag{1.31a}$$

$$\dot{\underline{p}} = -\frac{\partial H}{\partial \underline{q}}, \qquad \dot{\underline{q}} = \frac{\partial H}{\partial \underline{p}} \tag{1.31b}$$

and its equation of motion were first studied by Henon and Heiles. In order to detect chaos, they plotted the points in which the trajectory in phase space

$$\underline{x}(t) = [p_1(t), \; p_2(t), \; q_1(t), q_2(t)] \tag{1.32}$$

cuts the (p_1,p_2) - plane (here p_i and q_i are momenta and coordinates, respectively). This yeilds a Poincaré map as indicated below.

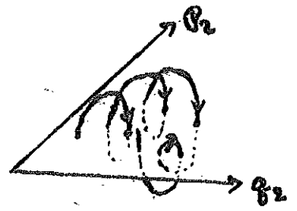

Fig. 1.12 Poincare section of a chaotic motion.

In general, the appearance of the poincare section for chaotic solution is that, it is space filling, but without a knowledge of chaotic attractor (understanding of their complicated structure) it is hard to explain. These attractors will be discussed at the end of Chapter 3,and Chapter 4 is fully devoted to their characterization. For the time being, we understand them to be a set in phase space, on to which all trajectories converge as $t \to \infty$ (that is to mean those trajectories which are in the basin of attraction).

On the other hand we recall that when the flow is very dissipative and results in a rapid contraction of areas, its Poincare section can practically be considered to be a set of points distributed along a curve (a line segment, an arc of a curve, etc.). In such a case one defines a coordinate x for each point on the curve, and studies how x varies with time. The Poincare map on this one dimensional graph is referred to as a 'first return map'. Even though the natural extension of the study of Poincare (sections) map is the analysis of first return map, i.e., the iteration

$$x_{n+1} = f(x_n) \tag{1.33}$$

in what follows this will be generalized to the study of dynamical systems as a whole.

1.3 The Description of Time Evolution-Dynamical Systems

In this section we will study, one dimensional noninvertible maps, two dymensional invertible maps, first order ordinary differential equations and very briefly ordinary partial differential equations.

1.3.1 One Dimensional Noninvertible Maps

To begin with, let us consider the one dimensional maps defined by (1.33)

$$x_{n+1} = F(x_n) \tag{1.33}$$

Where $F(x)$ is a scalar function. Here will be considered the case in which the sequence $x_0, x_1, x_2, \ldots$ generated by F is bounded. $P < x_n < Q$, for all n. One often says that such a sequence is chaotic, by which it is meant that the sequence has the following properties[2].

1) Sensitive dependance on initial conditions (i.e., if initial points x_0^α and x_0^ℓ are chosen very close to each other, the distance between their successive images under F initially diverges exponentially).

2) The average correlation function for a given sequence satisfies $C(m) \to 0$ as $m \to \infty$, where

$$C(m) = \lim_{N\to\infty} \frac{1}{N} \sum_{m=1}^{N} (x_n - \langle x\rangle)(x_{n+m} - \langle x\rangle) \tag{1.34a}$$

and

$$\langle x\rangle = \lim_{N\to\infty} \frac{1}{N} \sum_{n=1}^{N} x_n \tag{1.34b}$$

as given in (1.33).

3) The sequence is nonperiodic. There exist mathematical definitions[7] of chaotic F which will not be read here but the contents of these definitions are the same.

Now let us introduce the following two one dimensional maps, the so called tent map and quadratic map respectively.

$$F_1(x) = a(1-2\,|x-\tfrac{1}{2}|)\,,\ 0 < a \leq 1 \tag{1.35a}$$

$$F_2(x) = 4bx(1-x), \quad 0 < b \leq 1 \tag{1.35b}$$

where a and b are constants. For $0<(a,b) < 1$ the two functions map the unit interval onto itself, and we shall consider only this range of x(i.e., $0 < x_0 < 1$) for initial x_0). Both F_1 and F_2 are noninvertible, this is to say given $F(x_n)$ in terms of x_n one cannot solve for x_n. In other words it is possible to go forward in time but not bakcwards. This represents a basic difference with ordinary differential equations $\dot{x} = f(x)$, which may, in principle, be integrated either forward or backward in time.

First consider F_1. The two cases of interest are $0 < a < 1/2$ and $\frac{1}{2} < a < 1$, shown below.

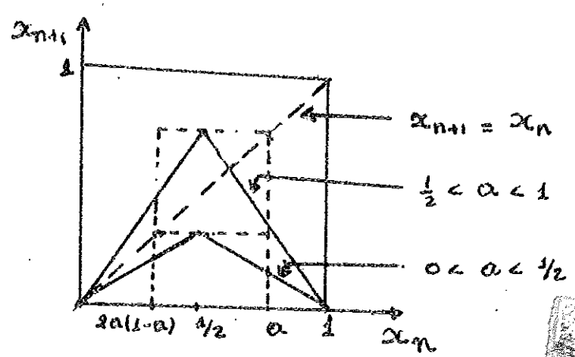

Fig. 1.13 Map F_1 Equation (1.35a)

As can be seen from Fig. (1.13), for $0 < a < \frac{1}{2}$ $x_{n+1} < x_n$, over the entire range, $F_1(x_n)$ lies below the line $x_{n+1} = x_n$. In this case it is clear that x_n converges to zero as n increases.

When $\frac{1}{2} < a < 1$, for an $x_0 \in [0,1]$, the sequence eventually becomes trapped in the interval $2a(1-a) < x < a$ through which it will wonder chaotically. As an illustration, let us consider the case when $a = 1$ for which the chaotic interval becomes $0 < x < 1$. In this case we may consider two steps:

i) a uniform stretching of the interval to twice its original length

ii) a folding in half of the stretched interval such that it has now its original length.

The stretching property leads to exponential separation of near by points and hence sensitivity dependence on initial conditions. The folding property keeps the generated sequance bounded, but also causes two different x_n points to be mapped into one x_{n-1} point.

(a) (b)

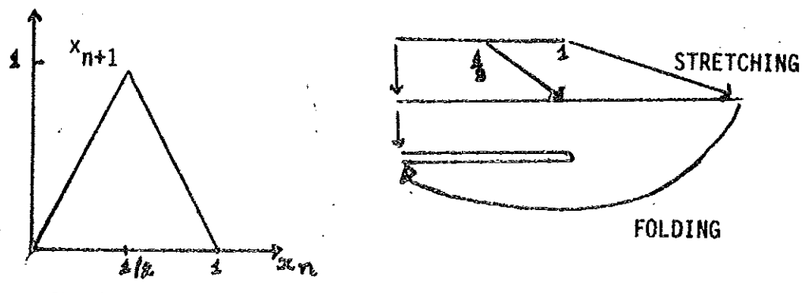

Fig. 1.14 a) f_1 map at a = 1

b) Illustration of the stretching and folding properties of F_1 at a = 1.

Conversely, for a general 1-D map, the distance between near by points to separate exponentially, it is necessary for the map to be stretched on the average. On the other hand to have the sequence remain bounded between 0 and 1 in the case of F_1, folding must take place. Hence, one concludes that in order for one-dimensional map to exhibit chaotic behavior, it should be non-invertible.

How do we understand the above properties for F_1 where $a < 1$ $(\frac{1}{2} < a \leq 1)$?

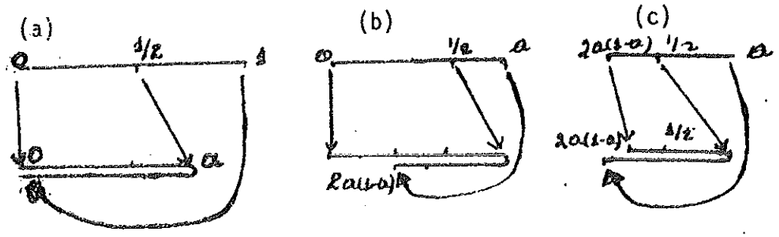

Fig. 1.15 Map of F_1 for $\frac{1}{2} < a < 1$ not to scale.

a) Mapping of the interval 0 to 1

b) 0 to a

c) 2a(1-a) to a

From figure above (a) it is seen that, after one application of F_1, there are no points in $a < x < 1$, in (b) we see that the interval 0 to 2a(1-a) is stretched but that no points are folded back onto it. Thus, any point in the interval $0 < x < 2a(1-a)$ will eventually leave the interval and never return. Therefore, the generated sequence is trapped in the interval $2a(1-a) < x < a$. Of course, many authors have derived the correlation function for the map under considerations[6,8] and the value is $C(m) = \frac{1}{12}\delta_{m,o}$, i.e. the sequence of iterates is delta correlated.

Before going to the discussion of F_2 (eq. 1.35b), let us review the concept of functional iteration. A random number generator is an example of a simple iteration scheme that has complex behavior. Such a scheme generates the next pseudorandom number by a definite transformtion upon the present pseudorandom number[9]. In other words a certain function is reevaluated successively to produce a sequence of such numbers. Thus, if f is the function and x_o is a starting number (or 'seed'), then $x_o, x_1, \ldots, x_n, \ldots$, where

$$\begin{aligned} x_1 &= f(x_o) \\ x_2 &= f(x_1) \\ &\vdots \end{aligned} \tag{1.36}$$

is a sequence of pseudorandom numbers. That is, they are generated by functional iteration. The n^{th} element in the sequence is

$$x_n = \underbrace{f(f(\ldots f(f(x_0))\ldots))}_{n \text{ times}} \tag{1.37}$$

where n is the total number of applications of f. A property of iterates worthy of mention is

$$f^n(f^m(x)) = f^m(f^n(x)) = f^{m+n}(x) \tag{1.38}$$

Since each expression is simply m+n applications of f. It is understood that

$$f^{(o)}(x) = x \tag{1.39}$$

Now let us turn to the consideration of F_2 of eq. (1.35b).

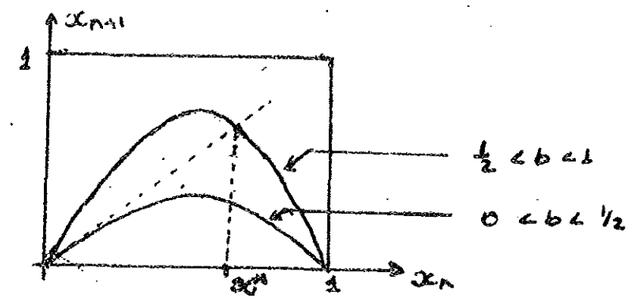

Fig. 1.16 The map F_2 Eq. (1.35b)

As b is varied, $x = o$ is always a fixed point. Indeed the fixed point equation for F(x) is

$$x^* = F(x^*) = 4b\, x^*(1-x^*)$$

gives us the two fixed points

$$x^* = o \text{ and } x^* = 1 - 1/4b$$

This means that the line $x_{n+1} = x_n$ intersects the map at $x_n = 0$ and $x_n = 1-(1/4b)$; i.e.; if the initial point is chosen to be a fixed point, then the successive application of the map leave it unmoved.

To see whether the fixed points are stable or not under small perturbation:

Let x^* be a fixed point, then $x^* = F(x^*)$, and consider a small perturbation from it

$$x_n = x^* + \sigma_n \tag{1.40}$$

but $x_{n+1} = F(x_n)$, and from this follows

$$x^* + \sigma_{n+1} = F(x^* + \sigma_n) \tag{1.41}$$

By Taylor-series expansion for small σ_n we get

$$F(x^* + \sigma_n) = F(x^*) + \frac{\partial F}{\partial x}\Big|_{x=x^*} \sigma_n + \frac{1}{2} \frac{\partial^2 F}{\partial x^2}\Big|_{x=x^*} \sigma_n^2 + \cdots$$

Hence, for small σ_n

$$F(x^* + \sigma_n) = F(x^*) + F'(x^*)\sigma_n = x^* + F'(x^*)\sigma_n$$

$$\Longrightarrow \quad x^* + \sigma_{n+1} = x^* + F'(x^*)\,\sigma_n$$

$$\Longrightarrow \quad \frac{\sigma_{n+1}}{\sigma_n} = F'(x^*) \tag{1.42}$$

Therefore, if $|F'(x^*)| > 1$, images under F of points near x^* successively move further away from it showing that x^* is unstable. On the other hand if $\left|\frac{\partial F}{\partial x}\right|_{x=x^*} < 1$ points near x^* converge to it, and x^* is stable. For instance, for F_2 of (1.35b).

$F'(0) = 4b$ and $x^* = 0$ is stable for $b < 1/4$. The fixed point $x^* = x$ first appears at $b = 1/4$, and simultaneously with its appearance, $x^* = 0$ loses its stability.

Consider the fixed point $x^* = 1 - 1/4b$

$$\begin{aligned} F(x^*) &= 2(1 - 2b) \\ |F'(x^*)| &= |2(1-2b)| < 1 \end{aligned} \tag{1.43}$$

This criteria will be met for the range of values $1/4 \leq b < 3/4$. Over this range x^* is stable. The natural question to ask is then what happens in the region $3/4 < b < 1$ for which both $x^* = 0$ and $x^* = 1 - 1/4b$ are unstable? It is observed that as b increases slightly beyond $b = 3/4$, F undergoes period doubling, that is to say, instead of having a stable cycle of period 1, the system has a stable cycle of period 2. i.e., the cycle contains two points. Another way of looking at the problem is by examining the map $x_{n+2} = F^2(x_n)$. Shown in figure below for b slightly below

(a) (b)

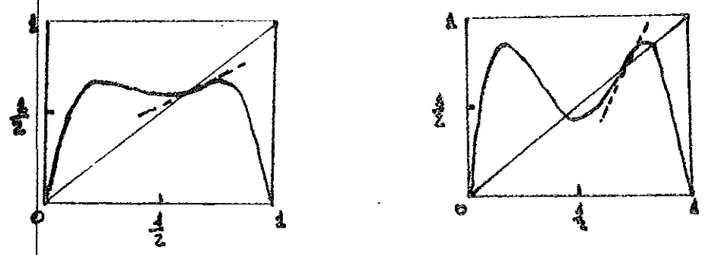

Fig. 1.17 x_{n+2} VS x_n for F_2 with (a) b = 0.678 and (b) b = 0.854. The dashed lines are the slope at $x = x^*$. The intersections of $x_{n+2} = x_n$ with $x_{n+2} = F_2^2(x_n)$ are $a_1 > x^* > a_2$. (See reference 3).

3/4 and for b slightly above 3/4. Values of x which recur every second iteration, i.e., in a series $a_1, a_2, a_1, a_2, \ldots$ are fixed points of F^2, $a_1 = F^2(a_1)$, and $a_2 = F^2(a_2)$, with $a_1 = F(a_2)$ and $a_2 = F(a_1)$. For the special case $a_1 = a_2$ a_1 will also be a fixed point of F itself. Now consider the stability of the sequence $a_1, a_2, a_1, a_2, \ldots$. Taking $x_n = a_1 + \sigma_n$, $x_{n+2} = a_1 + \sigma_{n+2}$ we have

$$a_1 + \sigma_{n+2} = F^2(a_1 + \sigma_n) = F[F(a_1 + \sigma_n)] \tag{1.44}$$

which, when Taylor-series expanded, yields

$$\frac{\sigma_{n+2}}{\sigma_n} = F'(a_1)\, F'(a_2) = F^{2\prime}(a_1) = F^{2\prime}(a_2) \tag{1.45}$$

Applying (1.45) to a fixed point of F, we have $F^{2'}(x^*) = [F'(x^*)]^2$. Thus, when x^* loses stability, the slope of $F^{(2)}$ at x^* becomes greater than one. Referring now to Fig.(1.17) for F_2 it is seen that, when this occurs, two new intersections of F_2^2 with $x_{n+2} = x_n$ a_1 and a_2 simultaneously appear. Furthermore, when this points appear, they intially have $F_2^2(a_1) = F^{2'}(a_2) = 1$ and the slope decreases as b is raised. Thus, the new fixed points of $F^{2'}$ are initially stable, and it is found that, when b slightly exceeds 3/4, the generated sequence converges to an alternating one $a_1, a_2, a_1, a_2, \ldots$. As b increases further, however, $F_2^{2'}(a_1) = F_2^{2'}(a_2)$ decreases; eventually past $b = 0.862, \ldots$, $F_2^{2'}(a_2)$ becomes less than minus one, and a_1, a_2 cycle becomes unstable. What happens next can be deduced, in an analogous way from the map $x_{n+4} = F_2^{2'}[F_2^2(x_n)] = F_2^{4'}(x_n)$, when the a_1, a_2 cycle loses stability, a stable four-point periodic cycle simultaneously appears; $a_3, a_4, a_5, a_6, a_3, a_4, a_5, a_6, \ldots$ which then gives way ("bifurcates") to an eight-point cycle, which then gives way to 16-point cycle, etc. Furthermore, the band of b values over which a given 2^k-point cycle is stable decreases geometrically with k, so that

$$\frac{b_k - b_{k-1}}{b_{k+1} - b_k} \longrightarrow 4.669201 \qquad (1.46)$$

For $k \to \infty$, where b_k is the value of b at the point where the 2^k-point cycle bifurcates to a 2^{k+1}-point cycle. Aslo $b_k \to 0.892$ for $n \to \infty$, that is, there is an accumulation point of an infinite number of bifurcations at $b_\infty = 0.892$. Feigenbaum derived[2,9,10] the above relation (Eq.(1.46)) using arguments based on scale invariance near b_∞ , and has also obtained other properties of the generated sequence for b near b_∞ . These properties apply independently of the

detailed functional form of the map as long as it has quadratic maximum as F_2. Thus, Eq.(1.46) apply to a wide class of maps.

Just past b the orbit generated by F_2 looks like a noisy cycle of periodicity 2^n with $n \to \infty$ as b approaches b_∞ from above. By a "noisy cycle periodicity 2^n" we mean that the orbit is confined to 2^n disjoint intervals in $1 > x > 0$ which it visits in a sequential order. Thus, the orbit always comes back to the same interval after a 2^n iteration. On the other hand, if one looks at the points generated by F^{2^n} with an initial condition in one of these intervals then the orbit looks completely chaotic in this interval. As b increases, these intervals merge in pairs so that a noisy 2^n cycle goes into a noisy 2^{n-1} cycle as b increases past a critical value $\bar{b}_n$. Also $\bar{b}_n$ obeys the same scaling low as (1.46). As b increases past $\bar{b}_1$, chaotic motion over a single connected band emerges.

In addition to the noisy 2^n cycles, narrow windows in b also exists within $b_\infty < b < 1$ for which the generated sequence is exactly periodic.

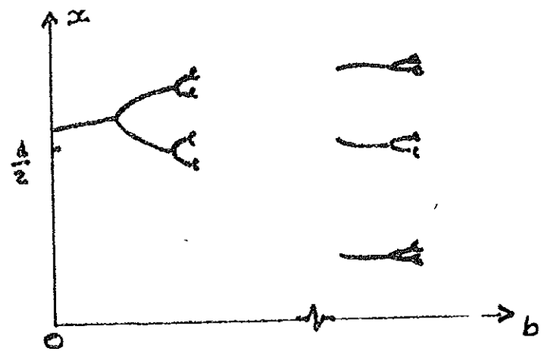

Fig. 1.18 Summary diagram for some of the bifurcations of $F^{(2)}$. The scale about the period $3x2^n$ cycles has been greatly expanded. (After E. Ott)

Generally, these periodic sequences appear with some period N and then

go through a sequence of period doubling bifurcations creating periods $2^n N$, with an accumulation point at $n \to \infty$ ending the particular periodic window. The widest such window is for $3x2^n$ periodic cycles, $0.9571 < b < 0.9624$. Other periodic windows are exceedingly narrow in b, and most of the range $b_\infty < b < 1$, appears to be chaotic. For values of b where numerically generated sequences appear to be chaotic, it is not, at present, known[2] whether they are truly chaotic, or whether, infact, are realy periodic but with exceedingly large periods and very long transisnts required to settle down. However, numerical works suggests that they are truly chaotic[10].

1.3.2 Two Dimensional Invertible Maps.

A general two-dimensional map can be written as:

$$x_{n+1} = f_1(x_n, y_n), \quad y_{n+1} = f_2(x_n, y_n) \tag{1.47}$$

The map is invertible if (1.47) can be solved uniquely for x_n and y_n as functions of x_{n+1} and y_{n+1}, $x_n = g_1(x_{n+1}, y_{n+1})$, $y_n = g_2(x_{n+1}, y_{n+1})$. That is, it is possible to go either backwards or forwards in time.

A two dimensional invertible map can easily be constructed from a one-dimensional noninvertible map as follows:

$$x_{n+1} = F(x_n) + y_n \tag{1.48a}$$

$$y_{n+1} = \beta x_n \tag{1.48b}$$

where f(x) is noninvertible. For $\beta = 0$. $y_n = 0$ and the noninvertible one dimensional map is recovered. However, as long as $\beta \neq 0$, no matter how small it is, the map (1.48) is invertible.

$$x_n = y_{n+1}/\beta \quad , \quad y_n = x_{n+1} - F(y_{n+1}/\beta)$$

It is of interest to compute the Jacobian of the map (1.48).

$$|J| = \begin{vmatrix} \frac{\partial x_{n+1}}{\partial x_n} & \frac{\partial x_{n+1}}{\partial y_n} \\ \frac{\partial y_{n+1}}{\partial x_n} & \frac{\partial y_{n+1}}{\partial y_n} \end{vmatrix} = -\beta$$

Thus, for $|\beta| < 1$ we see that areas will contract by the factor $|\beta|$ on each application of the mapping.

As a modification of (1.48) consider the following:

$$x_{n+1} = y_n - x_n^2 \tag{1.49a}$$

$$y_{n+1} = a + bx_n \tag{1.49b}$$

with $|b| < 1$, it contracts areas. Eq.(1.49) is interesting because it

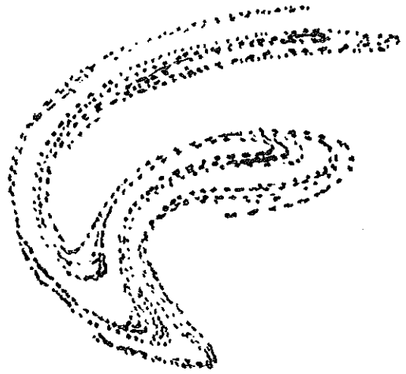

Fig. 1.19 The plotted points lie on a 'Chaotic' attractor of Duffing's equation. [From reference 9].

possesses a so called (strange) chaotic attractor. This means an attractor (as before) constructed by folding a curve repeatdely upon itself (figure above) with the consequent property that two initial points very near to one another, are in fact, very far from each other when the distance is measured along the folded attractor, which is the path they follow upon iteration. This means that after some iteration, they will soon be far apart in actual distance as well as when

measured along the attractor. This general mechanism gives a system highly sensitive dependence upon its initial conditions, and a truly statistical charactor. Since very small differences in initial conditions are magnified quickly, unless the initial conditions are known to infinite precision, all known knowledge is eroded to future ignorance. Now Eq. (1.49) enters into the early stage of statistical behavior through period doubling.

For a given system, if we denote by Λ_n the value of the parameter at which its period doubles for the n^{th} time, we find that the values of the parameter Λ_n converges to Λ_∞ (at which the motion is aperiodic) geometrically for large n, that is,

$$\Lambda_\infty - \Lambda_n \propto \sigma^{-n} \tag{1.50}$$

This is the generalization of Eq. (1.46) first discovered by Fiegenbaum. Of course

$$\sigma_n = \frac{\Lambda_{n+1} - \Lambda_n}{\Lambda_{n+2} - \Lambda_{n+1}} \longrightarrow 4.6692 \cdots \text{ as } n \to \infty$$

So here too σ is the rate of the onset of complexity. Another Fiegenbaum constant is α it is defined as

$\frac{d_n}{d_{n+1}} = -\alpha$, where d_n is the algebraic distance from $x = \frac{1}{2}$ to the nearest element of the attractor cycle of 2^n is the 2^n - cycle at Λ_n. So α scales this distance down in the 2^{n+1}-cycle at $n+1$:

$$\alpha = 2.502907875 \cdots$$

The above analysis is from one dimensional theory, it is also shown to hold here[2,9-10] (2-D case). That is, α is the rate at which the spacing of adjacent attractor points is vanishing. Indeed 1-D theory determines all behavior of (1.49) in the onset regime.

In fact, dimensionality is irrelevant. The same theory, the same numbers, etc., holds for iterations in N dimensions, provided that the system goes through period doubling. The basic, process, however period doubling occurs ad infinitum, is functional composition from one level to the next[9].

1.3.3 Systems of Ordinary Differential Equations and Partial Differential Equations

Here, we limit ourselves to the case of ordinary differential equations and at least we briefly review partial differential equations.

Now consider

$$\frac{dx_i}{dt} = f_i[x_1(t), x_2(t), x_3(t)], \quad i = 1,2,3 \qquad (1.51)$$

The system is autonomous because f_i does not depend explicitly on t but only on x_i. Alternately, a nonautonomous system of two coupled equations,

$$\frac{dx_1}{dt} = g_1(x_1, x_2, t), \quad \frac{dx_2}{dt} = g_2(x_1, x_2, t)$$

can be written in the form of (1.51) by defining

$$f_1 = g_1(x_1, x_2, x_3); \quad f_2 = g_2(x_1, x_2, x_3) \text{ and } f_3 = 1$$

We recall from section (1.2-2) that, the Poincare map represents a reduction of the systems dimension by one. With this in mind, consider a particular solution of (1.51) to generate an orbit in x_1, x_2, x_3 phase space. We assume that an appropriate surface has been chosen, and we study intersections of the orbit with this chosen surface.

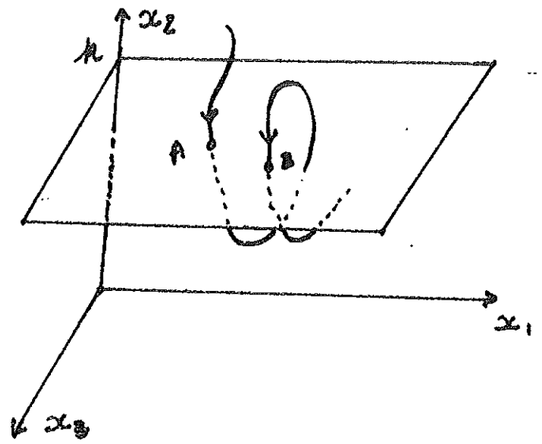

Fig. 1.20 Poincare Map of Eq. (1.51)

In Fig. 1.20, the chosen surface is the plane $x_2 = k$. Every time the orbit crosses the chosen surface in particular direction ($\frac{dx_2}{dt} < 0$ for the above figure). As has been said earlier we record the crossing point e.g. points A,B in figure 1.20, and it is clear that point A determines point B uniquely, also if one knows B,A is determined uniquely. Hence, the Poincare map in this illustration represents an invertible transformation of a point in the plane $x_2 = k$ into another point, i.e., it is an invertible two dimensional map.

As an example consider the following system of two nonautonomous ordinary differential equations

$$\frac{dp}{dt} = f(q) \sum_{n=-\infty}^{\infty} \delta(\omega t - 2n\pi) - \nu(p - p_o)$$

$$\frac{dq}{dt} = p$$

where $\delta(\psi)$ denotes the Dirac delta function of ψ. This can be written as three autonomous equations

$$\frac{dp}{dt} = f(q) \sum_{n=-\infty}^{\infty} \delta(\psi - 2n\pi) - \nu(p - p_0) \tag{1.52a}$$

$$\frac{dq}{dt} = p \tag{1.52b}$$

$$\frac{d\psi}{dt} = \omega \tag{1.52c}$$

We take the surface of section to be $\psi = 2m\pi - \varepsilon$ where $\varepsilon \to 0^+$. Defining $(p_m, q_m) = \lim_{\varepsilon \to 0^+} [p(t_m - \varepsilon), q(t_m - \varepsilon)]$, and $t_m = \frac{2m\pi}{\omega}$ Eqn.(1.52) yeild by simple integration, the following two dimensional map:

$$y_{m+1} = e^{\Gamma}[y_m + f(q_m)] \tag{1.53a}$$

$$q_{m+1} = q_m + (1-e^{\Gamma})\nu^{-1}[y_m + f(q_m)] + 2\pi p_0/\omega$$

where $\Gamma = 2\pi\nu/\omega$, and $y_m = P_m - P_0$. By a suitable choice of f(q) this two dimensional map may be reduced to that studied by Zaslaviskii*.

Now, we turn to a discussion of the evolution of phase-space volume as governed by (1.51). That is, we consider the volume V enclosed by some closed surface S in the x_1, x_2, x_3 phase space, and let the surface evolve by having each point on the surface follow an orbit generated by (1.51). Then for such a system by Lie derivative[5] we have

$$\frac{1}{V}\frac{dV}{dt} = \sum_i \frac{\partial \dot{x}_i}{\partial x_i} \tag{1.54}$$

where $\dot{x}_i \equiv \frac{dx_i}{dt} \equiv f_i$

In the special case where $\sum_i \frac{\partial f_i}{\partial x_i} = -k$ where k is a positive constant we have

$$V(t) = V(o)\, e^{-kt} \tag{1.55}$$

---

* Zaslaviskii studied the following map in 1978

$y_{n+1} = e^{\Gamma}(y_n + \varepsilon \cos(2\pi x_n)$

$x_{n+1} = \langle x_n + \frac{\Omega}{2\pi} + \frac{\alpha\Omega}{2\pi\Gamma}(1-e^{-\Gamma})y_n + \frac{k}{6}(1-e^{\Gamma})\cos(2\pi x_n)\rangle$ where $\langle \ldots \rangle$ denotes the fractional part of the argument $k = \alpha\varepsilon\Omega/2\pi$

From which we learn that, the phase-space volume shrinks exponentially in time. Many of the physical exampels yeilding a system of the form (1.51) that have been investigated for 'strange' attractors also happen to have a constant negative divergence, to which we shall restrict our discussion in the remainder of this section. At last we shall consider a more general case, without negative divergence.

The special case of three ordinarly outonomous differential equations with negative phase space flow divergence presents a very clear case for the necessity of introducing the concept of chaotic attractor. Since phase space volume contracts to zero in the limit of large time, it follows that any attractor must have zero volume. A natural assumption might be then that, the attractor would have to be a surface (2-D) a curve (1-D) or a point (0-D). However, non of these allows chaotic motion. In particular, not even the highest dimension of the above three possibilities (two) allows chaos. For example, for orbits within a finite section of a plane, the Poincare-Bendixson theorem[2,6] shows that the only possible attractor for the orbit must be either a point, a simple closed curve, or self interesecting closed curve. Thus, if one observes chaotic motion in the system (1.51), and if (1.51) has negative phase space divergence, then one is faced with something of a paradox. One way out is to realize that attractors with zero volume need not have dimension zero, one, or two, but, can in fact, have noninteger dimension. In particular, chaotic motion is possible if Eqn. (1.51) have attractor with dimension greater than two and less than three (the latter so that the volume of the attractor is zero). i.e., a chaotic attractor.

Examples

1. Lorenz's treatment of the Benard instability. This will be examined in some detail in Chapter two, but here we will state only the evolution equation of the system:

$$\frac{dX}{dt} = - X + Y$$

$$\frac{dY}{dt} = - XZ + r X - Y$$

$$\frac{dZ}{dt} = XY - bZ$$

2. Instability saturation by quadratically non-linear mode coupling[2].

A problem in plasma physics (and in other fields as well) is that of determining the nonlinear state resulting from a linearly unstable wave. An elementary process by which saturation can occur is that of resonant three-wave mode coupling of energy in the linearly unstable wave to two other waves which are linearly damped. The following normalized system of equations describes this process:

$$\frac{dC_1}{dt} = C_1 + C_2 C_3 \exp(i\sigma t)$$

$$\frac{dC_{2,3}}{dt} = - \gamma_{2,3} C_{2,3} - C_1 C^*_{3,2} \exp(i\sigma t)$$

where $C_i (i = 1,2,3)$ are time dependent complex wave amplitudes, C_i^* is the complex conjugate of C_i, times have been normalized to the growth rate of wave 1 (the higher frequency wave), σ represents the effect of a mismatch in the frequency resonance, and amplitudes have been normalized so that the coefficients of the nonlinear terms are one. Introducing $C_1 = a_1 e^{i\psi_1}$, $a_{2,3} e^{i\psi_{2,3}} = C_{2,3} e^{i\sigma t/2}$ and $\psi_1 + \psi_2 - (\psi_2 + \psi_3)$ where a_i and ψ_i

are real, the previous system gives four real equations for $a_{1,2,3}$ and ψ . These equations readily yeild

$$d(a_2^2 - a_3^2)/dt = -2(\gamma_2 a_2^2 - \gamma_3 a_3^2).$$

Thus, in special case $\gamma_2 = \gamma_3$, $a_2^2 - a_3^2$ decreases exponentially. Restricting consideration to $\gamma_2 = \gamma_3 \equiv \gamma$ and $a_2 = a_3$, the basic equations then becomes

$$\frac{da_1}{dt} = a_1 + a_2^2 \cos\psi$$

$$\frac{da_2}{dt} = -a_2(\gamma + a_1 \cos\psi)$$

$$\frac{d\psi}{dt} = -\sigma + a_1^{-1}(2a_1^2 - a_2^2), \sin\psi$$

The above system has been studied[2] for different values of γ and proven to have chaotic attractor for $\gamma = 15$.

It is natural to ask whether the phenomena revealed by the examples discussed above carry over to more complicated systems. In particular, what happens if the restriction of phase-space volume contraction is lifted and if the dimension of the system is larger than three? Furthermore, the above mentioned examples were meant as approximate models for phenomena which are more exactly described only by partial differential equations (PDE). PDE may often be thought of as infinite systems of ordinary differential equations; e.g., it is frequently possible[2,11-12] to expand the dependent variables of a PDE on an infinite discrete set of Fourier spatial modes and to derive an infinite set of coupled nonlinear ordinary differential equaions for the time dependence of the Fourier coefficients.

It seems clear that such more general systems might display the same characterstic phenomena as those examples discussed above, but could also reveal additional phenomena ruled out by the specific constraints adopted there. For example, in our discussion above for 3-D flow we pointed out that the dimension d of the attractor is such that, $3 > d > 2$. For higher dimensional flow chaotic attractors are possible with higher dimensions (see Chapter 4) e.g., one might have a chaotic attractor of dimension between 5 and 6 if a system of n differential equations with $n \geq 6$ were investigated (such chaotic attractors are hard to diagnose in actual situations). At any rate it seems reasonable to suppose that, as a parameter which characterizes the strength of destablizing forces in a system described by PDEs is cranked up (e.g., the Reynolds number), the general (although not uniform) tendency would be toward motion on attractors of increasing dimension. For example, a stable attracting point (zero-dimension attractor) might bifurcate to a periodic orbit (1-D attractor), which then give way to chaotic attractor via an infinite number of period doubling bifurcations. Whose dimension is between two and three which then becomes a chaotic attractor with dimension between three and four, etc. Another possible sequence might be a stationary point (zero dimensions) that bifurcates to a periodic orbit (1-D), which bifurcates to a doubly periodic orbit (2-D attractor formed by a surface of a torus) which then bifurcates to a chaotic attractor (dimension > 2)

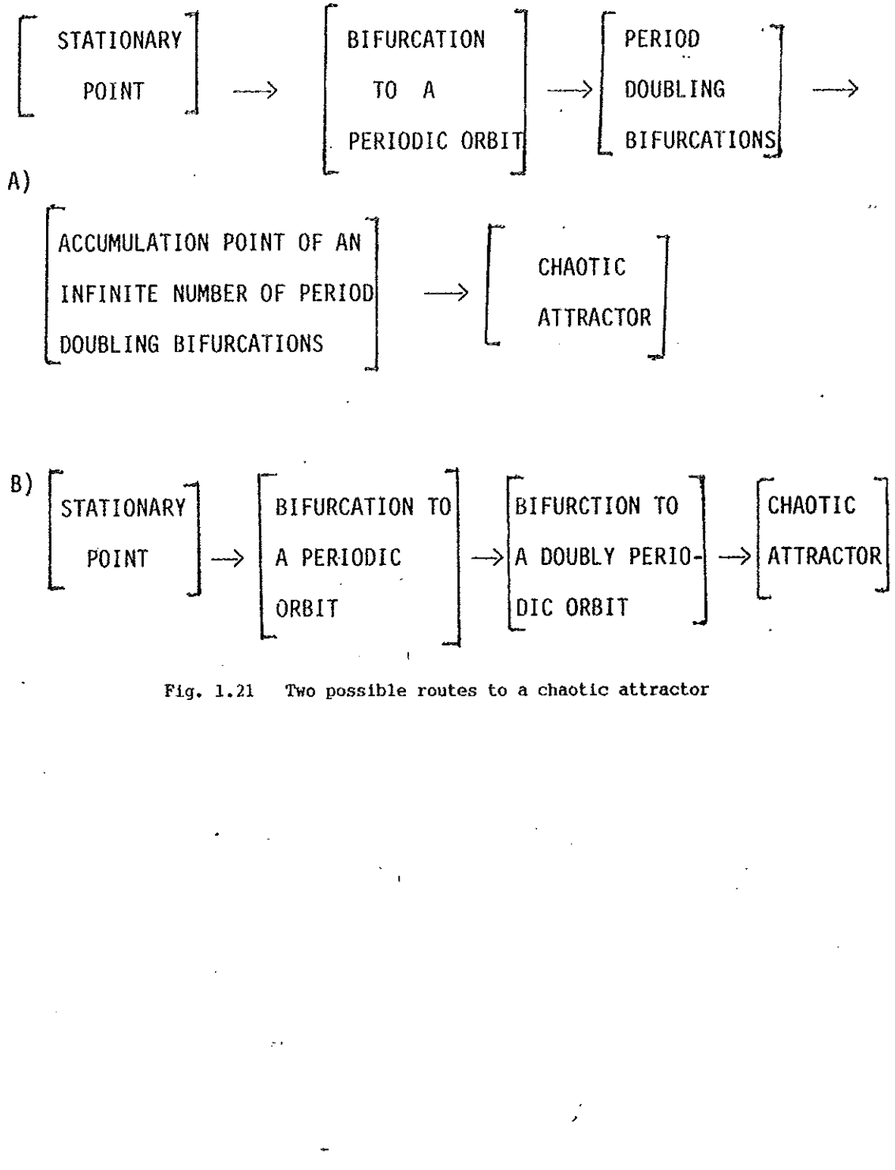

Fig. 1.21 Two possible routes to a chaotic attractor

CHAPTER 2

EXAMPLES OF DYNAMICAL SYSTEMS

2.0 Introduction

In the preceding chapter we have mentioned two examples of dynamical systmes, the Lorenz system and the one from plasma physics (instability saturation by quadratically nonlinear mode coupling). We have discussed the later problem in some detail and postponed the discussion of the former one to this chapter.

In order to further our discussion with deep insight into the problem at hand, in this chapter let us call upon three different experimental situations. First we shall consider an electromechanical apparatus with three degrees of freedom, consisting of a magnet placed in a magnetic field, which we will designate as a compass. This will be followed by a second example from hydrodynamics, the Lorenz treatment of Rayleigh-Benard convection, where we consider a horizontal layer of a fluid heated from below. Finally, our third example comes from chemistry; the famous Belousov-Zhabotinsky reaction.

2.1 The Compass

2.1.1 Description

The compass is simply a skillful realization of a parametric pendulum (a pendulum one of whose parameters varies with time[5]), allowing convenient and precise observation of the behavior of a system with three degrees of freedom. Like other similar devices, it was developed partly for purposes of demonstration. One of its most attractive aspects is that it offers the possibility of greately varying the

importance of friction. This permits the observation and analysis of the influence of energy dissipation as we go from a conservative or quasi-conservative situation (zero or negligible friction) to one which is more and more dissipative. [For schematic diagram of the experimental set up see reference 5].

A magnet, free to rotate about a vertical axis, is placed between two pairs of Helmholtz coils with horizontal perpendicular axes. An alternating sinusoidal current of angualr frequency ω and variable intensity is supplied to each pair of coils. Because the currents are in phase quadrature, these pairs of coils generate both a fixed magnetic field and a field which rotates about the axis of the magnet with the angualr frequency ω of the current. The rotating magnetic field tends to set the magnet into motion. Pick-up coils, perpendicular to the Helmholtz coils, are located near the magnet and detect its motion via the induced electromotive force. The signal collected $x(t)$ is a function of the instantaneous angular velocity of the magnet. After being amplified and filtered, the signal is sent to a Fourier analyzer which calculates the power spectrum.

Obtaining poincaré section of the phase trajectories is straight forward, since the compass is forced oscillator. Indeed, the rotation period of the imposed magnetic field provides a natural time interval for stroboscopy. So as to have a 2-D representation, two quantities are digitized and recorded simultaneously: x and $\dot{x}$ obtained analogically.

2.1.2 Evolution Equations

Consider the case in which friction is negligible. The forces applied set the compass in motion. Let θ be the angle between the magnet and a fixed direction in the horizontal plane (see Fig.(2.1)). Then, the variation of θ can be written as

$$J\ddot{\theta} + Me\ B_1 \sin\theta + Me\ B_0 \sin(\theta - \omega t) = 0 \qquad (2.1)$$

where J is the moment of inertia of the magnet, Me its magnetic moment, B_1 stationary induction and B_0 a rotating magnetic induction which rotates with angular velocity ω.

To make the equation dimensionless, let the magnetic fields be independent of the position of the magnet, and $M = Me\ B_1/(J\omega^2)$; and $P = Me\ B_0/J\omega^2$ and taking $1/\omega$ as the unit of time we arrive at

$$\ddot{\theta} + M \sin\theta + P \sin(\theta - t) = 0 \qquad (2.2)$$

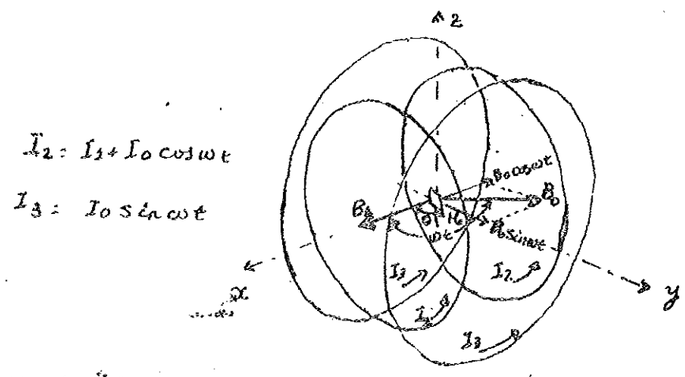

Fig. (2.1) Diagram of the arrangement of the magnet M with respect to the field producing coils.

The rotating magnetic field B_0 is produced by the two pairs of Helmholtz coils with perpendicular axes, supplied with sinusoidal currents. $I_0 \sin\omega t$ and $I_0 \cos\omega t$, respectively. The stationary magnetic field B_1 is produced by a constant electric current sent through one of the coil pairs (from reference 5).

In the presence of friction, which opposes motion and proportional to the speed the above equation can be written as

$$\ddot{\theta} + \alpha \dot{\theta} = - (M \sin \theta + \sin (\theta - t)) \qquad (2.3)$$

This is second order nonautonomous differential equation, equivalent to flow in R^3, and can be written as follows with the three variables y, θ, γ:

$$\dot{y} = - \alpha y - M \sin \theta - P \sin(\theta - \gamma) \qquad (2.4a)$$

$$\dot{\theta} = y \qquad (2.4b)$$

$$\dot{\gamma} = 1 \qquad (2.4c)$$

Thus, it is clear that we do have a nonlinear system with three degrees of freedom.Physically, the variable γ (related to ωt) represents the angle between the rotating magnetic field and a fixed direction fo the plane. This is why the solution is periodic of period 2π in units of $1/\omega$ - in the γ component.

2.2 Lorenz's Treatment of Rayleigh-Benard Convection

2.2.1 Description

The phenomena of thermal convection[5,12] occurs when the buoyancy force in a fluid due to externally imposed temperature gradients exceeds external frictional forces and the internal dissipation forces of the fluid. The buoyancy force occurs in most fluids because they expand when heated. Due to this expansion, the light hot fluid will rise and the cold heavy fluid will fall in an external gravitational field.

In order to study the phenomenon of thermal convection it is common to impose a temperature difference across a thin layer of fluid. If the fluid layer is thin enough that variation in material properties

of the fluid with hight can be ignored and large enough to avoid certain complicated effects due to boundaries, the convection pattern takes the form of two-dimensional rolls. Lord Rayleigh first studied

$a = H/\ell_x$

where ℓ_x is the length of the container

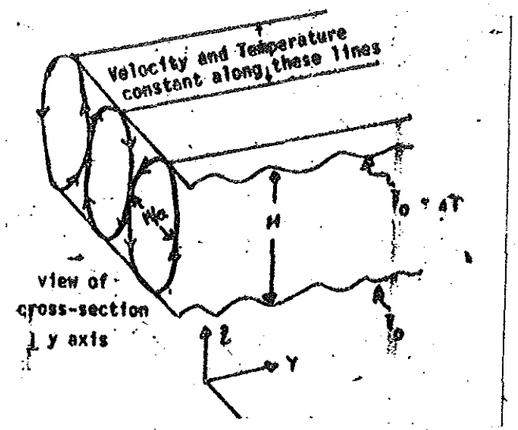

Fig. 2.2 Velocity and temperature fields in roll plan form for the Lorenz model.

this phenomena theoretically and calculated the temperature difference at which the rolls would form.

2.2.2 Evolution Equations

The equations describing the heated fluid pictured in Fig.2.2 are[12,14]

$$\frac{\partial u_i}{\partial t} + u_j \frac{\partial u_i}{\partial x_j} = g\epsilon\Delta T\, \delta_{i3} - \frac{1}{\rho}\frac{\partial p}{\partial x_i} + \nu\nabla^2 u_i \qquad (2.5a)$$

$$\frac{\partial T}{\partial t} + u_j \frac{\partial T}{\partial x_j} = k\nabla^2 T \qquad (2.5b)$$

$$\frac{\partial u_i}{\partial x_i} = 0 \qquad (2.5c)$$

In Eqn.(2.5), u_i is the i^{th} component of velocity, x_i is the i^{th} spatial coordinate ($i = 3$ being the vertical coordinate), t is the time, g is gravitational constant, ϵ is the coefficient of thermal expansion, ΔT is the difference between the temperature at a given

point and the average temperature of the fluid layer and k is the coefficient of thermal diffusivity.

This complicated equations have been treated in the typical way. First, suitable physical assumptions and approximations are made to simplify them as much as possible. This includes scaling and introduction of dimensionless variables. Next the temperature and velocity fields are expanded in a Fourier series expansion once suitable boundary conditions (rectangular box) have been established. Then, products of triginometric functions are replaced by sums using standard triginometric identities. Finally, the linear independence of the triginometric coefficients is used to relate time derivatives of the Fourier coefficients to nonlinear functions of these coefficients.

The convection equations of Saltzman: this is an alternative approach. The system studied by Rayleigh (i.e., the flow occuring in a layer of fluid of uniform depth H, when the temprature difference between the upper and lower surfaces is maintained at a constant value,) possesses a steady-state solution in which there is no motion, and the temperature varies linearly with depth. If this solution is unstable, convection should develop. In the case where all motions are parallel to the x-z plane, and no variations in the direction of the y-axis occur, the governing equations may be written as[11,13,14]

$$\frac{\partial}{\partial t}(\nabla^2\psi) = -\frac{\partial}{\partial(X,Z)}(\psi, \nabla^2\psi) + \nu\nabla^4\psi + g\varepsilon\frac{\partial\theta}{\partial X} \qquad (2.6a)$$

$$\frac{\partial\theta}{\partial t} = -\frac{\partial(\psi,\theta)}{\partial(X,Z)} + \frac{\Delta T}{H}\frac{\partial\psi}{\partial X} + k\nabla^2\theta \qquad (2.6b)$$

where ψ is the stream function ($\underline{u} = \underline{\nabla}\psi$) and $\theta = T(x,z,t) - T_{\bar{a}v}$ decreases linearly by ΔT between the bottom and top surfaces of the

fluid. The problem is most tractable when both the upper and lower boundaries are taken to be free, in which case ψ and $\nabla^2\psi$ vanish at both boundaries.

Rayleigh found that fields of motion of the form[11]

$$\psi = \psi_0 \sin(\pi a H^{-1} x) \sin(\pi H^{-1} z) \qquad (2.7a)$$

$$\theta = \theta_0 \cos(\pi a H^{-1} x) \cos(\pi H^{-1} z) \qquad (2.7b)$$

would develop if the quantity:

$$Ra = g \varepsilon H^3 \Delta T (\nu k)^{-1}$$

now called the Rayleigh number, exceeded a critical value

$$Rc = \pi^4 a^{-2} (1+a^2)^3$$

Saltzman[3] derived a set of ordinary differential equations by expanding ψ and θ in double Fourier series in x and z, with functions of t alone for coefficients and substituting these series into eqn.(2.6). His numerical studies shows that, of the coupled non-linear equations resulting from (2.6), independent of initial conditions, all but three of the Fourier coefficients involved in the expansion of θ and ψ quickly approached zero, and these three variables underwent irregular, apparently non periodic fluctuations.

To get the same results Lorenz trancated the Fourier series to include only three terms at the start. In doing so he introduced the following ansatz for the stream function and temperature difference[10,11,12],

$$\frac{a}{k(1+a^2)} \psi = \sqrt{2}\, X \sin(\pi a H^{-1} x) \sin(\pi H^{-1} z) \qquad (2.8a)$$

$$\pi R_c^{-1} R_a (\Delta T)^{-1} \theta = \sqrt{2}\, Y \cos(\pi a H^{-1} x) \cos(\pi H^{-1} z) - Z \sin(2\pi H^{-1} z) \qquad (2.8b)$$

After a little algebra one will find the following nonlinear equations (X, Y, Z are functions of time alone)

$$\dot{X} = -\sigma X + \sigma Y \tag{2.9a}$$

$$\dot{Y} = -XZ + rX - Y \tag{2.9b}$$

$$\dot{Z} = XY - bZ \tag{2.9c}$$

where $(\dot{}) \equiv \frac{d}{d\tau}$, $\tau = \pi^2 H^{-1}(1+a^2)kt$ $\sigma = \nu/k$ (known as Prandtl number) $r = R_c^{-1} R_a$ and $b = 4/(1+a^2)$.

These set of equations are known as Lorenz equations which describe the evolution of a fluid convection.

In these equations X is proportional to the intensity of the convective motion, while Y is proportional to the temperature difference between the ascending and descending currents, similar signs of X and Y denoting that warm fluid is rising and cold fluid is descending. The variable Z is proportional to the distortion of the vertical temperature profile from linearity, a positive value indicating that the strongest gradients occur near the boundaries.

Lorenz numerically considered the solution of (2.9) for a case in which $\sigma = 10$, $b = 8/3$ and $r = 24.74$. For these values of the parameter he obtained a chaotic solution. i.e., the solution will converge on to a strange attractor. This will be dealt with in the next chapter. Now as our last example we will discuss the Belousov-Zhabotinsky reaction from Chemistry.

2.3 The Belousov-Zhabotinsky Reaction

".... I asked in 1971 a chemist, specialist of these periodic reactions (chemical reactions that are periodic in time), if he thought that one would find chemical reactions with chaotic time dependence. He answered that if an experimentalist obtained a chaotic record in the study of a chemical reaction, he would throw away the record, saying that the experiment was unsuccessful...."

David Ruelle

2.3.1 Description

For about thirty years now, an oscillating reaction has been known to chemists. The oscillations have a period of the order of one minute and continue for perhaps an hour, until the reagents are exhausted. If reagents are added continuously, while reaction products are removed the oscillations proceed periodically forever. The reaction is roughly speaking, the oxidization of malonate by bromate, catalyzed by cerium. The experiment is easy to realize: here is the recipie[5,10,15]

H_2SO_4	1.5M	$C_2(SO_4)_3$	0.002M
$NaBrO_3$	0.08M	Ferroin	$3x10^{-4}M$
$CH_2(COOH)_2$	0.002M		

M means "molar", for instance $NaBrO_3$ (sodium bromate) occurs at the concentration of 0.08 moles per liter. Quantitative measurement imposes additional requirements. First of all, characterization of the dynamical regime requires that the regime be maintained for a sufficiently long time. Concretely, this means that an open reactor must be used, continually supplied with reactants and provided with

an overflow pipe. To keep the concentration of the species constant the mixture must be stirred rapidly and intensely. Finally, since the speed of these chemical reactions is sensitive to the temperature thermoregulation of the reactor is necessary. The progress of the reaction is followed by measuring one property of the medium.

2.3.2 Evolution Equations

A chemical reaction can be considered as a sequence of elementary steps, symbolized by

$$\nu_{ir}\, X_i \xrightarrow{k_r} \nu_{jr}\, X'_j, \quad \text{where,} \quad i,j = 1,\ldots,L$$

index of the L chemical species, $r = 1,\ldots,n$ index of the R elementary steps X_i: reactants; X'_j: products, ν_{ir}: molecularity of species i in step r, k_r: rate constant of step r.

In a homogeneous medium at constant volume, the variation in molar concentration $[X_\ell]$ of a species resulting from the reaction above are given by

$$\frac{d[X_\ell]}{dt} = \sum_{r=1}^{R} (\nu'_{\ell r} - \nu_{\ell r})\, k_r \prod_i [X_i]^{\nu_{ir}}, \quad \ell = 1,\ldots,L \qquad (2.10)$$

When the reaction takes place in an open reactor of volume V, fed by a volume flux J, each reactant enters with concentration $[X]_0$ and is evacuated through the overflow with its instantaneous concentration [X]. So one must add to the preceding equation the contribution due to transport:

$$[\dot{X}_\ell] = \sum_{r=1}^{R} (\nu'_{\ell r} - \nu_{\ell r}) k_r \prod_i [X_i]^{\nu_{ir}} + S/V([X_\ell]_0 - [X_\ell]), \quad \ell = 1\ldots,L \qquad (2.11)$$

This system of differential equations bears some resemblance to the equation of the Rayleigh-Benard instability. They are nonlinear.

equations, first order in time. Here the nonlinearity comes from interactions between chemical species ($\prod_i [X_i]^{\nu_{ir}}$).

To sum up, situations are not the same as they were twenty years-ago, as quoted at the begining of this section, chaotic records are not meant for the failure of the experiment. The study of this dynamical system shows that for some controlling parameters (J/V, for instance) the system is dissipative. This means that there is contraction of volume in phase space which the system occupies and it goes to zero as $t \to \infty$, meaning that trajectories converge on to a region of zero volume in the state space. The same is also true for the Lorenz system described in section (2.2). The study of this region of space, which we call an attractor, is the subject of the next chapter, where we study different types of attractors.

CHAPTER 3

DIFFERENT TYPES OF ATTRACTORS

3.1 Asymptotic Behavior of Dissipative Systems and the Simplest Attractors

Most of the ideas necessary for describing the time dependent behavior of dynamical systems have been introduced in the first two chapters. Let us summarize the main results. We want to analyze the evolution of arbitrary dissipative systems. The systems are assumed to be deterministic since they are described either by a continuous flow:

$$\frac{d}{dt}\underline{X}(t) = \underline{F}(\underline{X}(t)) \tag{3.1}$$

or by a discrete time mapping:

$$\underline{X}_{n+1} = \underline{f}(\underline{X}_n) \tag{3.2}$$

Where $\underline{X}$ is a vector in R^m $(m \geq 1)$. The function $\underline{F}$ contains one or several control parameters μ which express the constraint imposed by external world on the system under investigation. The constraint can be, for instance, the intensity of a magnetic field, the Rayleigh number, or the mean residence time: in a reactor. By changing a control parameter, it is possible to alter the behavior of the system. During the observation, the control parameter is kept (or assumed to be) constant.

It is remembered from chapter one that we have classified dynamical systems as to whether they conserve volume in phase space or not. We shall exclusively deal with the later one, dissipative systems, and we start now with the description of their attractors. Assume there is a finite volume V in state space ($\mathbb{R}^m$). Such that if $y \in V$ then $T^t y = X(y,t)$ is in V for all $t > o$. Since the flow T^t decreases volumes, the sets $T^t V$ decrease as $t \to \infty$ to a set

$$W = \bigcap_{t>o} T^t V \tag{3.3}$$

Thus, every solution curve starting at some $y \in V$ approaches W as $t \to \infty$. We can alternately say that if $y \in V/W$ then y is transient and the curve $T^t y$ will for some sufficently large t definitevely depart from y and converge to W. This is in sharp contrast with the situation encountered in nondissipative closed systems, where almost all curves $T^t y$ return infinitely often arbitrarily close to their initial state y. We shall not discuss the question of transience, although this is an interesting subject. Therefore, we consider only systems which have attained some sort of "internal equilibrium". In other words, we analyze the motion on W or on parts of W, assuming the orbits which tend to W but are not in it behave similarly to those in W, at least after a sufficient lapse of time. As we mentioned earlier, these parts of W will be called attractors, and studying attractors only amounts to neglecting transient behavior. Before reading the definition of attractors, it should be kept in mind that there is no universal agreement about what the best definition should be.

Definition

An attractor for the flow T^t is a compact set X satisfying

i) X is invariant under T^t: $T^t X = X$

ii) X has a shrinking neighborhood, i.e., there is an open neighborhood of U of X $U \supset X$ such that $T^t U \subset U$ for $t > o$ and $X = \bigcap_{t>o}^{t} U$

A good definition of an attractor needs another ingredient which generalizes the description of k separate attractors. This is fulfilled by the following requirement.

iii) The flow T^t on X is recurrent and indecomposable. Recurrent means T^t is no where transient on X: If U is an open set in V and if $U \cap V \neq \phi$, then there are arbitrarly many values of t such that $T^t \underline{x} \in X \cap U$ when $\underline{x} \in X \cap U$. Indecomposable means that X can not be split into two nontrivial closed invariant pieces.

If X is an attractor, its basin of attraction is defined to be the set of initial points $\underline{X}$ such that $T^t\underline{X}$ approaches X as $t \to \infty$. A flow can have several different attractors, each with its own basin of attraction. Mappings have even been constructed which have a (countably) infinite number of attractors. We will limit our treatment to the case of a single attractor.

In the sprit of what has been said above, one should arrive at a description of the nontransient behavior of dynamical systems by classifying their attractors and the motion on them. This aim is clearly felt throughout the literature on dynamical systems. One is, however, far from any complete classification of attractors, or even from a canonical choice of adequate classification criteria. What will be presented here is a more modest approach which will lead to a description of some non-trivial attractors, which have the additional feature that they arise as modifications of trivial attractors as an external parameter is changed. Thus, instead of considering a single problem, we deal with a one parameter family of problems:

$$\frac{d}{dt}\underline{x}(t) = \underline{F}_\mu(\underline{x}(t)); \quad \underline{x}(o) = \underline{y} \tag{3.4a}$$

or

$$\underline{x}_{n+1} = \underline{F}_\mu(\underline{x}_n), \; \underline{x}_o = \underline{y} \tag{3.4b}$$

where μ is the controlling parameter. It is assumed that μ stays

fixed during the whole duration of the experiment. We are interested in the changes of the attractors as μ is varied. In general, the attractor changes smoothly for small variations of the parameter.

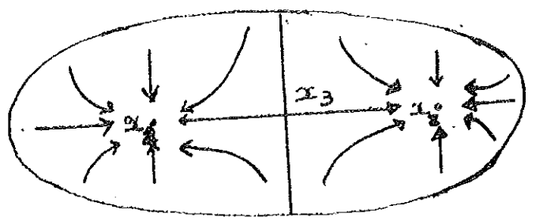

Fig. 3.1 Phase portrait illustrating two stable (x_1,x_2) and one unstable (x_3) fixed point. Here $H = \{x_1, x_2, x_3\}$

For example a fixed point (or a point attractor which is a solution that is independent of time i.e., a steady state, may move a little but as the parameter is varied or a stable limit cycle, a solution that is periodic in time, may change its shape and/or the time needed to complete a cycle (see Fig. 3.2).

Fig. 3.2 Phase portrait illustrating stable limit cycles

Sometimes, however, the topological nature of the attractor may change as the parameter crosses a point μ_0. One calls this a bifurcation point. For example in Fig. 3.3, the fixed (stable) point at μ_1 changes to a stable limit cycle at μ_2 (plus unstable fixed point).

Quite often a bifurcation is prompted by the crossing, of eigen values of the linearized flow at the fixed point (or periodic orbit) through the unit circle when the parameter passes through μ_B

Fig. 3.3 Phase portrait illustrating Hopf bifurcation

3.2 Limit Cycles, Simple Periodic Attractors

A periodic orbit (formerly elliptic) with variational equations whose solutions all decay to zero, i.e., the orbits near the periodic orbit are attracted to it is said to be simple periodic attractor. In a 'damped' system there is only one-trivial-attractor: the point of rest (at the origin). The origin sometimes be 'repelling', if its variational solutions become unbounded (see Fig. 3.3. The change of the controlling parameter made the origin unstable). If positive damping prevails further out in phase space we can have a periodic orbit in between approached by all orbits as $t \to \infty$. [For the method how to obtain these periodic orbits, see reference 16]. One example is the Van-der Pol equation:
$\ddot{y} - (1-y^2)\,\dot{y} + y = 0$ [see reference 5,16], and limit cycle.

3.3 Bifurcating Periodic Attractors

Here we find that one of the variational solutions of a simple attractor (limit cycle) of period m_2 becomes unbounded, as one

increases the magnitude of some parameter μ which plays a role similar to that of the 'Reynolds number' in fluid mechanics. At that point μ_1 a new attractor, with 2 loops-whence of period $2m_2$ splits off the old one which continues hyperbolic. At some higher point μ_2 the new attractor becomes hyperbolic itself and yet another attractor of period $4m_2$ splits off, etc. It has been found that the resulting sequence ('Feigenbaum sequence') $\{\mu_k\}$ converges rapidly, albeit at a different rate from the-conservative sequence [16,17]. Thus, near μ_1 there is a point μ_∞ at which the original simple attractor has bifurcated into an infinite number of branches (see sec.(1.30)). The hyperbolic branches of these tree converge to some limit orbit of 'infinite period', again at a rate different from the one for a conservative Feigenbaum. In reference 16, it is shown why the dissipative rates are the same for all values of the damping $|B|$ $(\neq 1)$ in

$$Y_{t+1} + BY_{t-1} = 2CY_t + 2Y_t^2 \qquad (3.5)$$

In particular it is shown that near the limit of each tree the local mapping converges to one described by a first-difference equation. Hence, Henon's mapping [18]

$$X_{t+1} = 1-aX_t^2 + bX_{t-1} \qquad (3.6)$$

and others all have the same Feigenbaum rates as the 'logistic equation'

$$X_{t+1} = aX_t(1-X_t) \qquad (3.7)$$

It is shown also why $B = \pm 1$ (conservative system) yield different rates. The literature on dissipative systems usually discusses the increasing sequence while the decreasing (mirror-) sequence is normally used in conservative systems. The period -1 and -2 attractors

are slightly simpler for the decreasing sequence whence our choice of standard form Eqn. 3.5 with

$$C_1 \leq C_0 \ , \ C_1 = -(\tfrac{1+B}{2}) \ , \ C_0 = (\tfrac{1+B}{2}) \qquad (3.8)$$

As the parameter μ we choose[16]:

$$1 + B - C,$$

where $|B| > 1$, after some simple algebraic manipulation, one obtains an equation which has period doubling attractors if we let $t \to -\infty$. Hence, as one lets $t \to +\infty$, there are trees of 'period-doubling repellers' for $|B| > 1$. [For definition of repellers see reference 7]. Before bifurcation each such repeller has a variational equation[10,16] with two unbounded basis solutions ($B \neq 0$). The existence of a 'chaotic attractor', which is the topic of the next section, therefore, implies the existence of a 'chaotic repeller' at 1/B. Repelling quasi-random orbits and Cantor sets have been discovered.

4 Strange (or Chaotic) Attractors

4.0 Introduction

What kind of attractor is associated with a regime whose Fourier spectrum contains a broad band? The Soviet Physicist Landau first tried to answer this question in 1944[5,6]. In trying to explain how a fluid makes a transition from laminar to turbulent flow when the Reynolds number R_e is increased, he advanced the following idea, now known as Landau theory of turbulence. Above the first instability threshold, the fluid velocity, which previously was constant in time (laminar flow), becomes periodic: it is modulated with a certain frequency f_1. Then if we continue to increase R_e, the periodic regime inturn loses its stability. A quasi periodic regime sets in

via the appearance of a second frequency f_2, incommensurate with f_1. Continuing this chain of reasoning, we expect to see other frequencies f_3, f_4,..., f_r in succession, by destabilization of more and more oscillatroy modes. For r large enough, turbulent flow would then be obtained. And since the distinction between a Fourier spectrum composed of many neighboring peaks, and a continuous spectrum is, in practice, the attractor of a turbulent flow would therefore be a torus T^r of sufficiently high dimension r.

The corrolary to this alluringly simple hypothesis is that only systems with a large number of degrees of freedom can display chaotic behavior, since the dimension of the phase space must be greater than that of the attractor. Yet, we know today, mainly from numerical simulations of three-dimensional flows, that this conclusion is false: three degrees of freedom suffice to give rise to a chaotic regime, in the sense described above.

It is to Ruelle and Takens that we owe the break through in 1971 of having introduced attractors topologically different from the torus, which they named 'Strange Attractors', and of having shown that such attractors could be important in physical problems, including hydrodynamical turbulence. The name 'strange (chaotic) attractor' refers to their unsual properties, the most crucial being sensitivity to initial conditions. By virtue of sensitivity to initial conditions, any two initially close trajectories on the attractor eventually diverge from one another. Their divergence (averaged over short time intervals) even increases exponentially with time.

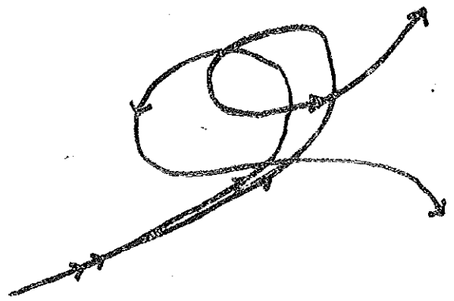

Fig. 3.4 Sensitivity to initial conditions
Regardless of their initial proximity, two neighbouring phase trajectories on a strange attractor always diverge.

From Fig. 3.4, one learns that the slightest imprecision in specifying the initial conditions will prevent us from deciding which will be the trajectory followed by the system, and therefore, from making other than a statistical prediction on the long-term future of the system. This leads to a highly non-trivial result: the impossibility of predicting the behavior of certain determinstic flow with only three degrees of freedom!

3.4.1 Characterization of Chaotic Regime

Let us review what has been said about chaotic regime, in chapter 1, with a view towards deducing properties of attractors associated with chaotic behavior.

In a chaotic regime, the power spectrum of one of the variables X of the dynamical system contains a continuous part, expressing the fact that the evolution of X is disordered and erratic. To estimate the amount of disorder it is useful to introduce a function measuring the resemblance of X at time t with itself at a later time $t + \tau$.

This quantity $C(\tau)$ is obtained by averaging over a large number of products $X(t) \cdot X(\tau + t)$:

$$C(\tau) = \frac{1}{t_2 - t_1} \int_{t_1}^{t_2} X(t) \cdot X(t+\tau)\, dt \qquad (3.9a)$$

or in more condensed notation

$$C(\tau) = \langle X(t) \cdot X(t+\tau) \rangle \qquad (3.9b)$$

by varying the interval τ we construct $C(\tau)$, called the temporal autocorrelation function. According to eqn. 1.21 $C(\tau)$ is the Fourier transform of the power spectrum. If $X(t)$ is a constant, periodic or quasi-periodic then the power spectrum is composed of distinct peaks. Therefore, $C(\tau)$ will remain non-zero as $\tau \to \infty$.

Fig. 3.5 A chaotic regime [from reference 5]
a) Form of the power spectrum S(f)
b) Form of the autocorrelation function $C(\tau)$

A periodic (or quasi-periodic) signal resembles itself at later times. This means that the behavior of the system is predictable since knowledge of it for a sufficiently long time enables us to construct it at all later times by simple comparison. On the other hand, in chaotic regime where the power spectrum includes a continuous part, $C(\tau)$ necessarily tends to zero as $\tau \to \infty$ (see Fig. 3.5). The autocorrelation function has a finite support: the resemblance

of the signal with itself in time diminishes, and even disappears for times that are sufficiently far apart. It follows that no finite interval of observation of X(t) suffices to predict its future behavior. The chaotic regime is intrinsically unpredictable, by progressive loss of self-similarity, or loss of memory of initial conditions. In fact, this reflects only insensitivity to initial conditions and an impoverishment of the original information since many initial states outside of the attractor merge on the attractor. But when we speak of loss of memory of initial conditions in a chaotic regime, we mean that a set of imperceptibly different initial states on the attractor lead, in an unpredictable way, to many final states; in a way, information has not been lost, but rather gained. A crucial consequence on the dynamics is this: two trajectories that are initially very close will diverge, resulting in loss of all resemblance after a finite time (see Fig. 3.4). Conversely, if a regime is represented by an attractor on which near by trajectories diverge, then the regime is chaotic. This very important property of amplification (in fact exponential amplification) of errors or of initial uncertainity in a chaotic regime is called sensitivity to initial conditions

3.4.2 Properties of Chaotic Attractors

The idea of an attractor exhibiting sensitivity dependence to initial conditions is highly nonintutive. This is probably the explanation for the late discovery of chaos with a small number of degrees of freedom: determinstic chaos. The paradox resides in the apparent contradiction, which implies the convergence of trajectories, and sensitivity to initial conditions which implies their divergence.

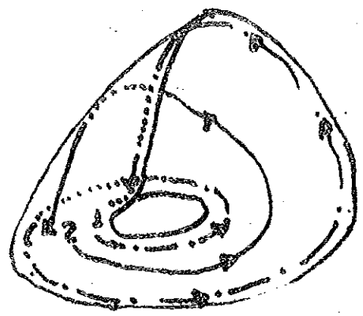

Fig. 3.6 Schematic representation of the divergence of two trajectories in a three dimensional phase space. The neighboring trajectories 1 and 2 emerge from the horizontal plane 'cross' without intersecting and return to the spiral. These curves are drawn on a simplified view of the Rösseler attractor. (From reference 5)

But the divergence of trajectories merely sets a lower bound on the attractor's dimension (dimensions will be discussed in chapter 4).

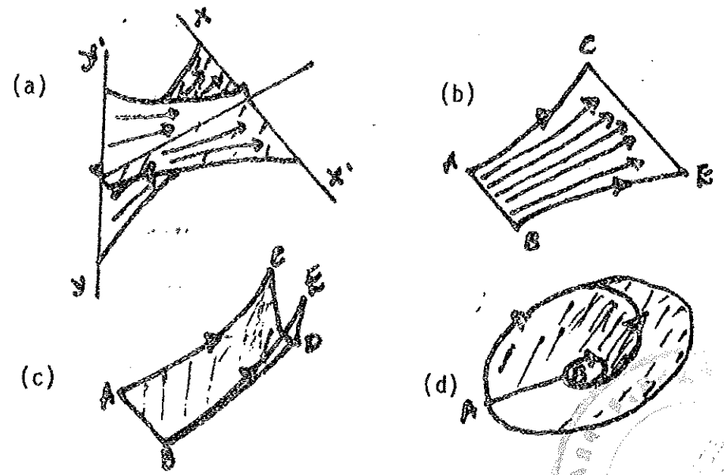

Fig. 3.7 Stages in construction of a chaotic attractor. (From reference 5)

To understand the origins of such a flow, imagine a three dimensional flow, diverging in the XX' direction and converging in the perpendicular direction YY' (see Fig. 3.7a). A set of initial conditions will lead to a quasi-two-dimensional sheet ABEC exhibiting the divergence of trajectories required for SIC (sensitivity to initial conditions) (see Fig. 3.7b). The stretching operation should not continue for ever, it should be followed by folding so that the flow will remain in a bounded three dimensional space. When the sheet's width has been elongated by some factor ($CE = m\,A\,B, m > 1$), CE is folded in two along CDE (Fig. 3.7c); then, the 'end' CD is connected up with the 'beginning' AB (Fig. 3.7d). We have thus constructed a 3-D flow exhibiting SIC in a finite space.

We see that in a 3-D phase space, the conflicting demands on attraction and sensitivity to initial conditions (SIC) are reconciled via the concept of hyperbolicity: attraction takes place in one direction, while divergence occurs in another. In figure 3.8 we show a plane perpendicular to the mean direction of the flow. The point O is called hyperbolic by geometric analogy. Along the sheet, i.e., in the XX' direction trajectories diverge from O, while in the perpendicular direction YY', the trajectories approach O. Of the two axes, the points move along curves which when projected onto the plane of Fig. 3.8 resemble hyperbolas.

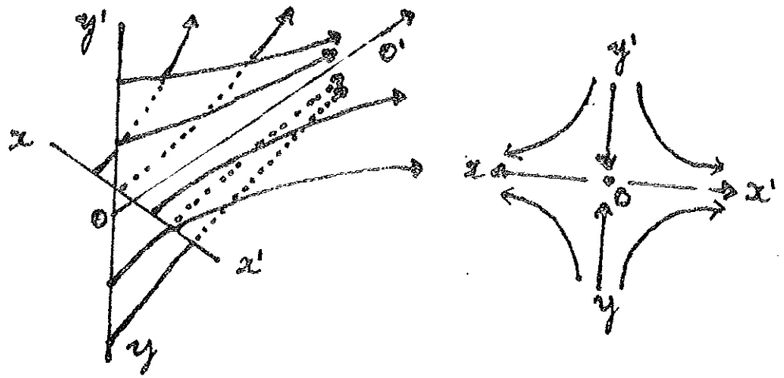

Fig. 3.8 Illustration of hyperbolicity

a) The bold curves are the divergent trajectories and the finer curves, the convergent trajectories. O O' is the direction of the mean flow, x x' the dilating and, y y' the contracting direction.

b) A projection of the flow onto a plane perpendicular to the direction O O'. The surface containing the convergent trajectories - here the plane y y' O O' - is called the stable manifold, while the surface containing the divergent trajectories - here the plane x x' O O' - is called unstable manifold.

Thus, there now exists a counterbalance to attraction, which destroys information: divergence which creates it. Having concluded that sensitivity to initial conditions requires that the dimension d of the attractor satisfy $d > 2$, one might at this point ask if a 3-D flow exhibits SIC. The question arises because in a dissipative system (i.e., system in which an attractor exists), volume in phase space contracts as time increases (see Chapter 1). The volume of the attractor must therefore be zero, which in a 3-D phase space implies $d < 3$. An attractor capable of representing chaotic regime must be such that $2 < d < 3$. This condition would seem to preclude the existence of such attractors, if we refer to Euclidean dimension, which is necessarily an integer. Nevertheless, we encounter attractors verifying the condition $2 < d < 3$. They have among other curious

properties, a non integer dimension, called fractal dimension (see Chapter 4).

Synopsis:

A dissipative dynamical system can became chaotic if the phase space has dimension D such that $D \geq 3$. This chaos - with a smaller number of degrees of freedom - is due to SIC of trajectories on strange (chaotic) attractors. The essential properties of chaotic attractors are:

i) It is an attractor.

ii) Pairs of neighboring trajectories diverge on it.

iii) Its dimension d is fractal.

1.3 Examples of Chaotic Attractors

- Chaotic Attractors in Nature

To describe the system which they encounter physicists, chemists, biologists, etc. use difference equations or differential equations in the case of continuous time. One should not underestimate the amount of idealization implied by such a description. Certain parameters are selected as variables[15] $x_1, x_2, \ldots, x_m$. Others are ignored. Idealization is a basic ingredient of all natural sciences, and one must show that the natural system which he considers obeys determinstic laws of the type (1.4) or (1.8) with a good approximation. He may then look for chaotic attractors, either by the direct study of experimental results, or by computer simulation. In this manner, the 'Chaos' which occur in certain phenomena becomes understandable, and it may be hoped that this understanding will lead to practical applications.

We shall now discuss some examples of chaotic attractors.

The Lorenz Attractor

In chapter two we have described the Bênard convection, and the evolution equations were

$$\dot{X} = -\sigma X + \sigma Y$$
$$\dot{Y} = -XZ + rX - Y$$
$$\dot{Z} = XY - bZ$$

These are the Lorenz's equations which describe the evolution of a fluid convection [11,12,13,15], [a horizontal fluid layer heated from below]. The warmer fluid at the bottom is lighter. It tends to rise, creating convection currents. If the heating is sufficiently intense, convection takes place, in an irregular, turbulent manner.

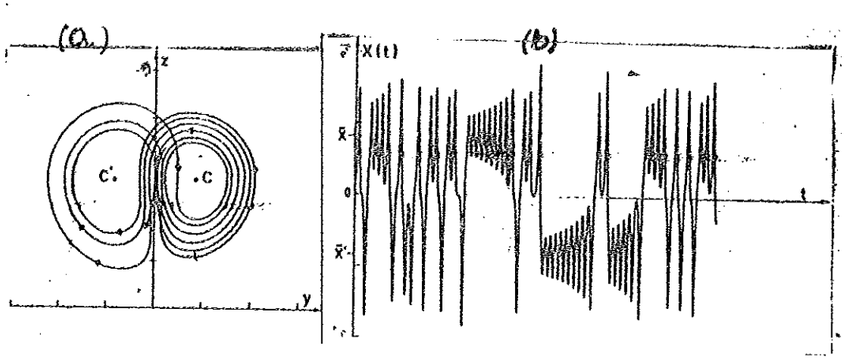

Fig. 3.9 The Lorenz Attractor

a) Projection of part of a trajectory onto the plane (Y,Z) of the phase space for r = 28 C and C' are unstable fixed points. [From reference 11]

b) Graph of X(t) for r = 28. Note the disordered evolution, some times about a mean value $\bar{X}$, and some times about another value $\bar{X}'$ (X and X' are the X coordinates of the unstable fixed points C and C' respectively). [From reference 5].

This phenomenan takes place for instance in the Earth atmosphere, and since it has sensitive dependence on initial conditions, it is understandable that meteorologists can not predict the state of the atmosphere with prediction a long time in advance. The work of E. Lorenz thus gives some theoretical excuse to the well known unreliability of weather forcasts.

Let us calculate the rate of change of volume with time for the Lorenz system:

From Chapter 1

$$\frac{1}{V}\frac{dv}{dt} = \sum_i \frac{\partial \dot{X}_i}{\partial X_i}$$

$\Longrightarrow \frac{1}{V}\frac{dv}{dt} = -(\sigma + b + 1)$, for Lorenz system.

For $\sigma = 10$ and $b = 8/3$,

$V = V(0)\, e^{-41/3t}$.

Thus, the system is highly dissipative. Once more let us return to Fig. 3.9a. Evidently, the orbits spirals outward from one of the points C or C' until it exceeds some critical distnace from the origin, at which point it starts spiraling about the other point. If one were to make a sequential list of the number of circuits the solution makes around one point before it switches to the other point, the sequence would appear to be chaotic. By examination of the solution, Lorenz has deduced that the orbit appears to be confined to a surface. Actually this apparent "surface" must have some small thickness, inside of which is embedded the more complicated structure of the chaotic attractor. In fact if one were to

pass a line through this surface normal to it, one would find that the intersection of the line with the surface is a set of dimension $0 < d < 1$. However, since the thickness of the chaotic attractor is small, presence of structure in this intersection would only be visible upon magnification, and unmagnified, it would appear to be a point.

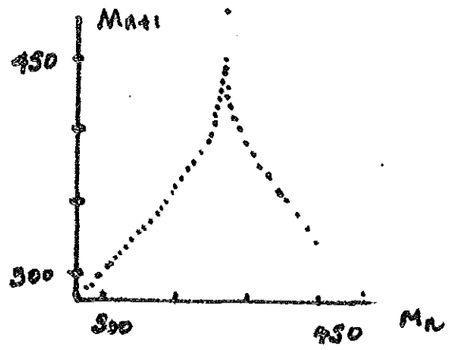

Fig. 3.10 First return map of the Lorenz model graph of $M_{n+1} = f(M_n)$
Where M_i are successive maxima of Z for r = 28.
[From reference 11].

From Fig. 3.10 it is clear that an approximate one dimensional map is generated. As has been seen in chapter one, the map is chaotic since $\left|\frac{dM_{n+1}}{dM_n}\right| > 1$. [For further discussion of Lorenz attractor see references 2 and 11].

The magnetism of the earth perhaps gives an example of a chaotic attractor. It is knwon that the Earth's magentic field reverses itself at irregular intervals. This phenomenon occured at least sixteen times in the last four million years[15]. Geophysicists have written "dynamo equations" with chaotic solutions which describe irregular changes of direction of a magnetic field. There is however as yet no quantitative satisfactory theory.

- Ecologists have studied nonperiodic models in population dynamics. If m species have, in the year t + 1, population $x_1(t+1),\ldots,$ $x_m(t+1)$, determined by the difference equation of the form

$$\underline{X}_{n+1} = \underline{F}(\underline{X}_n)$$

in terms of the population in the year t, one may expect chaotic attractos to occur. In fact, already, for m = 1, the equation

$$\underline{X}_{n+1} = R\, \underline{X}_{n+1}(1-\underline{X}_n)$$

gives rise to nonperiodic behavior[19].

To conclude this list of examples, which is far from complete, we will mention a dynamical system of vital interest to every one of us: the heart. The normal cardiac regime is periodic, but there are many non-periodic pathologies (like ventricular fibrillation) which lead to the steady state of death. It seems that great medical benefit might be derived from computer studies of a realistic mathematical model which would reproduce the various cardiac dynamical regimes. [For further detail discussions of this last example see references 20 and 21].

CHAPTER 4

CHARACTERIZATION OF CHAOTIC ATTRACTORS

Introduction

A chaotic attractor can be quantitatively characterized by its metric properties (giving rise to static, time independent invarients) or by dynamical invarients describing details of the temporal evolution of the considered system[8].

The most commonly used invarients in the later context are the Lyapunov exponents and the dynamical entropy (Kolmogroff entropy) of the system. We shall discuss these concepts in sec. 4.2.2. The metric properties of an attractor can be described by the dimensions of the attractor. More exactly one can define a continuous spectrum of dimensions by means of generalized information treatment. These shall be delt with in sec. 4.2.1.

The attractor of a dynamical system can easily be obtained if the coupled differential equations for the relevant variables of the system are known. However, in many experimental situations neither the relevant variables nor even their total number are known, so that the attractor of the system is not a priori accessible. In this case, the attractor can be reconstructed in an artificial phase space, if a time series of one single variable is measured. The embedding theorem of Takens ensures that the attractor can be reliably reconstructed in the limit of a sufficiently large dimension $d \to \infty$ of the artificial phase space. This reconstruction method will be discussed in sec. 4.3.

Finally, some experimental illustration of chaotic attractors, from different disciplines will be reviewed in sec. 4.4. Now to start with as chaotic attractors are fractals, we shall quickly review the concept of fractal dimension.

4.1 Fractal Dimension

What is a fractal? For us, for now, it is a subset of space. Whereas the space is simple, the fractal subset may be geometrically complicated[23]. Fractals were introduced by Mandlbrot as a generic term converging all kinds of Cantor-like objects. All these objects idealy have uncountably many substructures that are either identical (self-similar) or alike, except for scaling[24].

How big is a fractal? When are two fractals similar to one another in some sense? There are various numbers associated with fractals which can be used to compare them. They are generally referred to as 'fractal dimensions'. They are attempts to quantify a subjective feeling which we have about how densely the fractal occupies the metric space in which it lies. Fractal dimensions provide an objective means for comparing fractals.

Fractal dimensions are important because they can be defined in connection with real world data, and they can be measured approximately by means of experiments. For example one can measure fractal dimension of the coastline of Great Britain; its value is about 1.2. Fractal dimensions can be attached to[23] clouds, trees, coastlines, feathers, networks of neurons in the body, dust in the air at an instant in time, the clothes you are wearing, the distribution of frequencies of light reflected by a flower, the wrinkled surface of the sea during a storm and chaotic attractors of chaotic dynamical systems.

Let $(\mathbb{X}, d)$ denote a complete metric space. Let $A \in H(\mathbb{X})$ be a non-empty compact subset of $\mathbb{X}$. Assume $\epsilon > 0$, and let $B(x,\epsilon)$ denote the

closed ball of radius ε, and center at a point $x \in \mathbb{X}$. We wish to define an integer $N(A,\varepsilon)$ to be the least number of closed balls of radius ε needed to cover the set A. i.e.;

$N(A,\varepsilon)$ = smallest positive integer such that

$$A \subset \bigcup_{n=1}^{M} B(x_n, \varepsilon) \tag{4.1}$$

for some set of distinct points $\{x_n : n = 1,2,\ldots,M\} \subset$. The intutive idea behind fractal dimension is that a set A has fractal dimension D if:

$N(A,\varepsilon) = C\varepsilon^{-D}$ for some constant C solving for D we obtain

$$D = \frac{\ell n[N(A,\varepsilon)] - \ell nC}{\ell n(1/\varepsilon)} \tag{4.2}$$

In this equation one can see that, $\ell nc/\ell n(1/\varepsilon) \to 0$ as $\varepsilon \to 0$. This leads us to the following definition:

Definition:

Let $A \in H(\mathbb{X})$ where $(\mathbb{X},d)$ is a metric space. For each $\varepsilon > 0$ let $N(A,\varepsilon)$ denote the smallest number of closed balls of radius $\varepsilon > 0$ needed to cover A. If

$$D = \lim_{\varepsilon \to 0} \frac{\ell n[N(A,\varepsilon)]}{\ell n(1/\varepsilon)} \tag{4.3}$$

exists, then D is said to be fractal dimension of A.

Note that this definition gives the usual topological dimension for simple curves (for instance, $D(A) = 0$ if $A = \{a\} / a \in \mathbb{X}$, if a denotes the line segment $[0,1]$ then $D(A) = 1$, etc).

Theorem. Let $A \in H(\mathbb{X})$ where $(\mathbb{X},d)$ is a metric space. Let $\varepsilon_n = cr^n$ for real numbers $0 < r < 1$ and $c > 0$, and integers $n = 1,2,3,\ldots$.

If $$D = \lim_{n\to\infty} \left\{ \frac{\ell n[N(A.\varepsilon_n)]}{\ell n(1/\varepsilon_n)} \right\} \qquad (4.4)$$

then A has fractal dimension D.

Proof: see reference 23.

Example: Sierpinski carpet

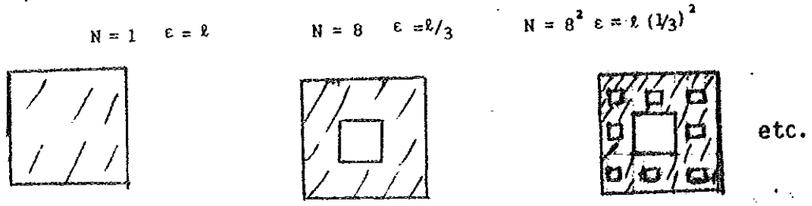

etc.

Fig. 4.1 Some stages in the construction of the Sierpinski carpet.

Let $C = 1/\ell > 0$ then $\varepsilon_n = Cr^n = \frac{\ell^2}{\ell} 3^{-n}$ so that,

$$D = \lim_{n\to\infty} \frac{n\,\ell n\,8}{n\,\ell n\,3} = \frac{\ell n\,8}{\ell n\,3} = 1.893$$

Having completed this digression on fractal dimension, we return to our main goal, which is to study chaotic attractors, in particular, their characterization.

4.2 Characterization of Chaotic Attractors

4.2.1 Dimensions of Chaotic Attractors

For most purposes one may think of the natural measure of an attractor as follows: For subset S of the phase space and an initial condition $\underline{X}$ in the basin of attraction of the attractor, we define $\mu(\underline{X},S)$ as the fraction of time the trajectory originating at $\underline{X}$ spends in S in the limit that the length of the trajectory goes to infinity. If $\mu(\underline{X},S)$ is the same for almost every $\underline{X}$ in the basin of attraction, then we denote this value $\mu(S)$ and say that μ is the natural measure

of the attractor. Henceforth, we assume that the attractor has a natural measure. In particular, this means that the attractor is ergodic (i.e., cannot be split into two disjoint pieces that each have positive natural measure and are invariant under application of $\underline{F}$).

Let $B(\epsilon,\underline{X})$, denote a d-dimensional ball of radius ϵ centered at point $\underline{x}$ on an attractor embedded in the d-dimensional phase space of the dynamical system being considered. Then the pointwise dimension (at the point $\underline{x}$) of the attractor is defined as

$$D_p(\underline{x}) = \lim_{\epsilon \to 0} \frac{\ell n \mu[B(\epsilon,\underline{x})]}{\ell n \epsilon}$$

or

$$\mu[B(\epsilon,\underline{x})] \sim \epsilon^{D_p(\underline{x})} \qquad (4.5)$$

For almost every point with respect to the natural measure on the attractor, $D_p(\underline{x})$ takes on a common value and is equal to the information dimension[23] (this will be defined later on). This is, to say, the set of points on the chaotic attractor for which $D_p(\underline{x})$ is not the common value may be covered with a set of d-dimensional cubes of varying sizes which together contain an arbitrarily small amount of the natural measure of the attractor. For example a chaotic attractor orbits embedded within it, and, it has been shown that[25], $D_p(\underline{x})$ with $\underline{x}$ on one of these periodic orbits does not take on the typical values. The periodic points, however, are countable and so have zero measure.

Consider the zero measure set of points $\underline{x}$ for which $D_p(\underline{x})$ is not typical (i.e., is not the common value assumed at almost every $\underline{x}$ on the attractor) and taking the map to be two dimensional (d = 2) one

obtains the following result. Let j be an index labeling the fixed points of the n times iterated map $\underline{F}^n$. (The components of a period n orbit are fixed points of $\underline{F}^n$)[25]. Assume that the Jacobian matrix of $\underline{F}^n$ at fixed point j has one unstable direction and one stable direction. Then for any point $\underline{x}$ on the unstable manifold of fixed point j of $\underline{F}^n$,

$$D_p(\underline{x}) = 1 - \frac{\lambda_{1j}}{\lambda_{2j}} \qquad (4.6)$$

where $\lambda_{1j} > 1$ and $\lambda_{2j} < 1$ are magnitudes of the unstable and stable eigenvalues of the Jacobian matrix of $\underline{F}^n$. Since points on different periodic orbits typically have different eigenvalues, $D_p(\underline{x})$ will clearly be different for different periodic orbits and hence will not be the typical $D_p(\underline{x})$. [See reference 25 for how to obtain (4.6)].

Spectrum of Dimensions:

Here we define the spectrum of dimensions[6,8,25,26]

$$D_q = \frac{1}{q-1} \lim_{\varepsilon \to 0} \frac{\ell n \sum_{i=1}^{N(\varepsilon)} P_i^q}{\ell n\, \varepsilon} \qquad (4.7)$$

where the attractor is covered with $N(\varepsilon)$ d-dimensional cubes from a grid of unit length , and P_i the natural measure of the attractor in the i^{th} cube. Taking the limit $q \to 1$ eqn.(4.7) yeilds

$$D_1 = \lim_{\varepsilon \to 0} \frac{\sum_i P_i \ell n P_i}{\ell n\, \varepsilon} \qquad (4.8)$$

which is called the information dimension of the attractor. It is D_1 which is the common value assumed by $D_p(\underline{x})$ for almost all $\underline{x}$ with respect to the natural measure on the attractor. We may think of the information dimension as the capacity dimension of the smallest set which contains most of the natural measure of the attractor.

As q is increased past 1, the contribution of the sum $\sum_i P_i^q$ from a relatively few boxes with very little of the total attractor measure but with larger P_i than typical becomes relatively more important. Similarly as q is decreased from one, the contribution from low probability boxes begins to be more important. For instance, when q = 0 eqn.(4.7) gives

$$D_0 = \lim_{\epsilon \to 0} \frac{\ell n N(\epsilon)}{\ell n \epsilon} \tag{4.9}$$

which is identical to eqn.(4.3), known as fractal, box counting or capacity dimension of the attractor. Note that all boxes on the attractor contribute democratically to D_0 no matter what their natural measure P_i is. Since low-probability boxes containing very little of total natural measure on the attractor may be vastly more numerous than those required to cover most of the natural measure on the attractor, we have, for some typical chaotic attractors[27]

$$D_0 > D_1$$

Now let us discuss another dimension of attractor, the Hausdorff (or Hausdorff-Bescovitch) dimension. To define the Hausdorff dimension we cover the attractor with d-dimensional cubes of variable edge length ϵ_i[23,25], all of which we restrict to be no bigger than some value ϵ ($\epsilon_i \leq \epsilon$). We then form the quantity

$$\Gamma_H(D, \epsilon, \{\epsilon_i\}) = \sum_i \epsilon_i^D \tag{4.10}$$

Next the covering of cubes is optimized so as to make the sum $\sum_i \epsilon_i^D$, minimum,

$$\Gamma_H(D,\epsilon) = \{\inf_{\epsilon_i}\} \sum_i \epsilon_i^D \tag{4.11}$$

where the infimum is taken over all possible collections of cubes that cover the attractor subject to the constraint $\epsilon_i \leq \epsilon$. Finally,

the limit $\varepsilon \to 0$ is taken,

$$\Gamma_H(D) = \lim_{\varepsilon \to 0} \Gamma_H(D, \varepsilon) \tag{4.12}$$

The quantity $\Gamma_H(D)$ can be shown to be either zero or infinity except at a critical value of D. This critical value defines the Hausdorff dimension which we denote D_H.

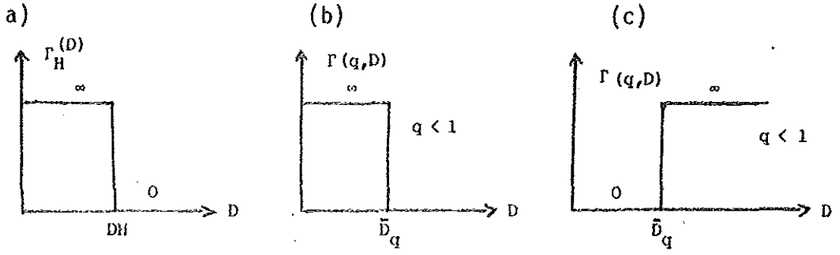

Fig. 4.2 (a) $\Gamma_H(D)$ V_S D_H (b) $\Gamma(q,D)$ for $q < 1$ (c) $\Gamma(q,D)$ for $q > 1$.

The capacity dimension D_0 and the Hausdorff dimension are closely related. In particular, if we do not optimize over the covering, but instead use a cubic grid covering of fixed length ε, then all the ε_i in (4.10) are equal to ε and we have

$$\Gamma_H^{(grid)}(D, \varepsilon) = N(\varepsilon)\, \varepsilon^D \tag{4.13}$$

[$\Gamma(q,D) = 0$ for $(q-1)D < (q-1)\tilde{D}_q$, and $\Gamma(q,D) = \infty$ for $(q-1)D > (q-1)\tilde{D}_q$ cf. Figs. 4.2(b) and 4.2(c)].

Again say that we do not optimize over coverings, but instead use a cubic grid, of basic length ε, then $\varepsilon_i = \varepsilon$ and we have $\sum_i p_i^q / \varepsilon_i \approx \varepsilon^{-\tau} \sum_i p_i^q$. From eqn.(4.7) $\sum_i p_i^q \sim \varepsilon^{(q-1)D_q}$ and hence $\sum_i p_i^q / \varepsilon_i^\tau \sim \varepsilon^{(q-1)(D_q - D)}$ which in the limit $\varepsilon \to 0$, pass from 0 to ∞ $D = D_q$. Since in this the optimization over coverings, prescribed in

eqn.(4.15), is not done, the quantity D_q defined by eqns.(4.14) to (4.16) is necessarily less than or equal to D_q,

$$D_q' \leq D_q \tag{4.17}$$

However, as for the Hausdorff and capacity dimensions, it is to be expected that, in practice, the equality in (4.17) typically holds for chaotic attractors.

Halsey et al[22], consider the set of $\underline{x}$ values such that $D_p(\underline{x}) = \alpha$ and they denote the Hausdorff dimension of this set by $f(\alpha)$. They show that D_q can be explicitly obtained from the dimensions $f(\alpha)$ via the formulas,

$$\frac{df(\alpha)}{d\alpha} = q \tag{4.18a}$$

$$(q-1)D_q = [q\alpha(q) - f(\alpha(q))] \tag{4.18b}$$

The corelation integral

Numerical determination of the dimensions D_q by covering the phase space with a set of boxes of volume ε^d and counting the number of iterates which lie in a certain cell is rather cumbersome and, in fact, impossible for attractors of higher dimensions. However, the special case $q = 2$ of (4.4) is much simpler. In this case the correlation dimension

$$D_2 = \lim_{\varepsilon \to 0} \frac{\ell n\left(\sum_{j=0}^{N(\varepsilon)} P_i^2\right)}{\ell n\, \varepsilon} \tag{4.19}$$

can be determined from the correlation integral

$$C(\varepsilon) = \lim_{T \to \infty} \frac{1}{T^2} \sum_{i,j}^{T} \theta[\ell - |\underline{x}_i - \underline{x}_j|] \tag{4.20}$$

This in turn can be directly evaluated for series of iterates.

D_2 is related to $C(\varepsilon)$ via

$\sum_{i=0}^{N(\varepsilon)} P_i^2$ = the probability that two points of the attractor lie within a cell ε^d

= the probability that two points at the attractor are separated by a distance smaller than ε.

$$= \lim_{T\to\infty} \frac{1}{T^2} \sum_{i,j} \theta[\varepsilon - |\underline{x}_i - \underline{x}_j|]$$

$$= C(\varepsilon) = \text{correlation integral} \qquad (4.21)$$

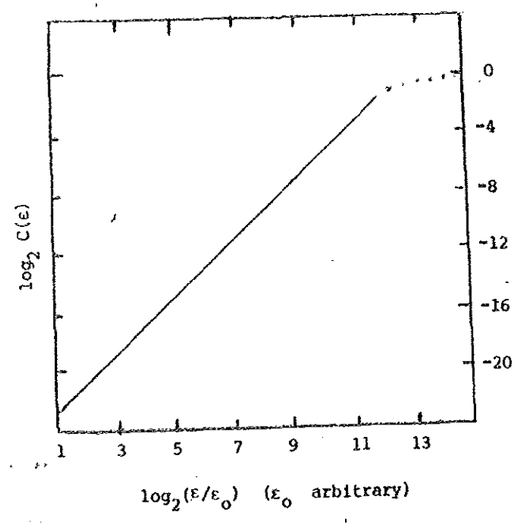

Fig. 4.3 $\log_2 C(\varepsilon)$ vs $\log_2 \varepsilon$ for the Lorenz system. The slope yields $D_2 = 2.05$ (From reference 27).

Here the Heaviside function $\theta(\varepsilon - |\underline{x}_i - \underline{x}_j|)$ serves to count how many pairs of points $(\underline{x}_i, \underline{x}_j)$ fall within the distance ε.

The procedure of Grossberger and procaccia has been recently extended to a calculation of dimension of arbitrary order q by a corresponding correlation integral $C_q(\varepsilon)^{2\theta}$,

$$C_q(\varepsilon) = \lim_{\varepsilon \to 0} \left[\frac{1}{N} \sum_{i=1}^{N} \left[\frac{1}{N} \sum_{j=1}^{N} \theta'\varepsilon - |\underline{x}_i - \underline{x}_j|\right]^{q-1}\right]^{\frac{1}{q-1}} \qquad (4.22)$$

using this correlation integral, the dimension of order q is given by

$$D_q = \lim_{\varepsilon \to 0} \frac{\ell n\, C_q(\theta)}{\ell n\, \varepsilon} \qquad (4.23)$$

For the case q = 2, the exponents of both summations in eqn.(4.22) are equal to one. This situation considerably facilitates the numerical work. For $q \neq 2$ the calculation is more involved since each individual sum has to be raised to the corresponding power. However, the increase in numerical effort is tolerable, particularly compared with the computing time required for direct box counting algorithms[8,23].

The spectrum of dimensions D_q using eqn.(4.23) contains more detailed information about the metric properties of the attractor than each single dimension does. This is understandable as at different order of different subsets on the attractor become dominant in the determination of D_q and C_q. Intuitively, the variation of q provides a scan through all degrees of point density existing along the trajectory.

4.2.2 The Lyapunov Exponent and Kolmogroff Entropy

A more quantitative measure of a chaotic regime comes from determination of the largest Lyapunov exponent. We will not discuss the algorithms for determining[5] this exponent from experimental data, since they are not yet operational but, the concept will be briefly discussed in here.

Another important measure by which chaotic motion (in an arbitrary-dimensional phase space) can be characterized is the Kolmogroff entropy. In this section we will discuss how this measure can be estimated from a chaotic signal, and its relation to the Lyapunov exponent.

The Lyapunov Exponent

We have seen in chapter 1 that adjacent points become separated under the action of a map

$$X_{n+1} = f(x_n) \tag{4.24}$$

which leads to chaotic motion. The Lyapunov exponent $\lambda(x_0)$ measures this exponential separation as shown in Fig.4.4.

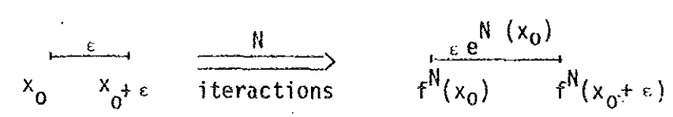

Fig. 4.4 Definition of the Lyapunov exponent.

From Fig. 4.4 we obtain

$$\varepsilon e^{N\lambda(x_0)} = \left| f^N(x_0) - f^N(x_0+\varepsilon) \right|$$

$$\Longrightarrow \lambda(x_0) = \lim_{N\to\infty} \frac{1}{N} \ln \left| \frac{df^N(x_0)}{dx_0} \right| \tag{4.25}$$

This means that $e^{\lambda(x_0)}$ is the average factor by which the distance between closely adjacent points becomes stretched after one iteration.

The Lyapunov exponent also measures the average loss of information after one iteration. In order to see this we use the chain rule in (4.25).

$$\frac{d\, f^2(x_0)}{d\, x_0} = \frac{d}{d x_0} f(f(x_0)) = \frac{d\, f(f(x_0))}{d x_0} = \frac{df(x_1)}{d x_0} \quad \frac{df(x_0)}{d x_0}$$

where $x_1 = f(x_0)$

$$\therefore \quad \frac{df^N(x_0)}{d x_0} = \prod_{i=0}^{N-1} \frac{df(x_i)}{d x_0} \tag{4.26}$$

Now the Lyapunov exponent can be written as:

$$\lambda(x_0) = \lim_{N\to\infty} \frac{1}{N} \sum_{i=0}^{N-1} \ell n \left| f'(x_i) \right| \tag{4.27}$$

where $f'(x_i) = \frac{df(x_i)}{d x_0}$

suppose the domain of $f(x_n)$ be [0,1]. Let us separate this interval into n equal intervals and assume that a point x_0 can occur with equal probability of 1/n in each interval. We want to answer the question, what is the loss of information after one iteration with a linear map? By learning which interval contains x_0 we gain the information [6].

$$I_0 = - \sum_{i=1}^{n} \frac{1}{n} \log_2 n = \log_2 n \tag{4.28}$$

If we decrease n the information I_0 is reduced and it becomes zero for n = 1.

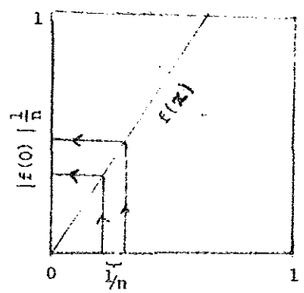

Fig. 4.5 Increase of an interval 1/n by a linear map.

It is shown in Fig.4.5 that a linear map f(x) changes the length of an interval by a factor $a = |f'(0)|$. The corresponding decrease of resolution leads to a loss of information after the mapping[6].

$$\Delta I = \sum_{i=1}^{n/a} a/n \log_2 a/n + \sum_{i=1}^{n} \frac{1}{n} \log 1/n$$

$$= - \log_2 a = - \log_2 |f'(0)| \qquad (4.29)$$

Generalizing this expression to a situation where $|f'(x)|$ varies from point to point and averaging over many iterations leads to the following expression:

$$\Delta I = - \lim_{N \to \infty} \frac{1}{N} \sum_{i=1}^{N-1} \log_2 |f'(x_i)|$$

This can be written as

$$\Delta I = - (\ell n 2)^{-1} \cdot \left[\lim_{N \to \infty} \frac{1}{N} \sum_{i=1}^{N-1} \ell n |f'(x_i)| \right] ,$$

but the quantity in the square brackets is simply $\lambda(x_0)$. Hence,

$$\lambda (x_0) = \ell n_2 |\Delta I| \qquad (4.30)$$

The Kolmogrov Entropy.

Before we introduce the Kolmogroff entropy it is useful to recall that the thermodynamic entropy S measures the disorder in a given system.

More precisely, the entropy S, which can be expressed as $S \propto - \sum_i P_i \ell n P_i$, where $\{P_i\}$ are the probabilities of finding the system in states $\{i\}$,

measures, according to Shanon et al[6], the information needed to locate the system in a certain state i^*, i.e., S is a measure of our ignorance about the system.

Let us get back to the Kolmogroff entropy, which we are interested in. Consider a dynamical system with N degrees of freedom. Suppose that N- dimensional phase space is partitioned to boxes of size ε^N. Suppose that there is an attractor in phase space and that the trajectory $\underline{x}(t)$ is in the basin of attraction. The state of the system is now measured at intervals of time τ. Let $P(i_1,\ldots,i_d)$ be the joint probability that $\underline{x}(t=\tau)$ is in box i_1, $\underline{x}(t=2\tau)$ is in box i_2, and $\underline{x}(t=d\tau)$ is in box i_d. The Kolmogrov entropy is then

$$K = -\lim_{\tau\to 0} \lim_{\varepsilon\to 0} \lim_{d\to\infty} \frac{1}{d\tau} \sum_{i_1,\ldots,i_d} P(i_1,\ldots,i_d) \ln P(i_1,\ldots,i_d) \quad (4.31)$$

The limit $\varepsilon \to 0$ (which is to be taken after $d\to\infty$) makes K independent of the particular partition. For maps with discrete time steps $\tau = 1$, the limit $\tau \to 0$ is omitted.

In table 4.1 we see that K is indeed a useful measure of chaos. It becomes zero for regular motion, infinite in random systems, a constant greater than zero if the system displays deterministic chaos.

In the following we will see the connection of K to the Lyapunov exponents.

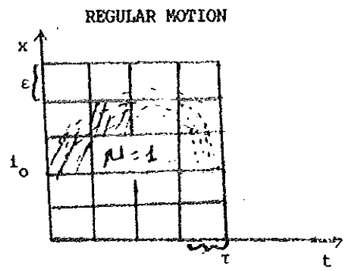

Initially adjacent points stay adjacent

$P(i_0) = \varepsilon$, $P(i_0,i_1) = \varepsilon.1$

$\Longrightarrow$ K = 0

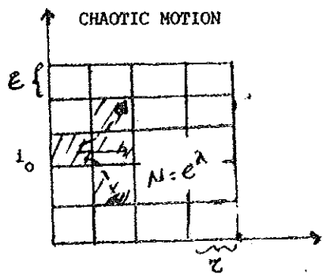

Initially adjacent become exponentially separated $P(i_0) = \lambda$, $P(i_0,i_j) = \varepsilon e^{-\lambda}$

$K = \lambda > 0$

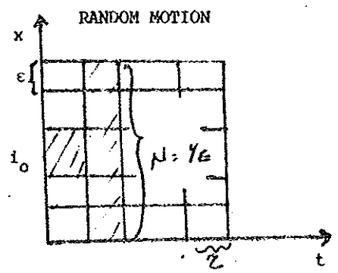

Initially adjacent points are distributed with equal probability over all newly alowed intervals

$P(i_0) = \varepsilon$, $P(i_0,i_1) = \frac{P(i_0)}{N}$

$\Longrightarrow K \propto -\ell n\, \varepsilon \to \infty$

Table 4.1 K entropies for (one-dimensional) regular, chaotic R Random motion. Here we assumed for simplicity that

a) $P(i_o, i_1)$ factorizes into $P(i_o)\frac{1}{N}$ where N is the number of possible new intervals which evolves from i_o and

b) $K_{d+1} - K_d = K_1 - K_o$ for all d where

$K_d \equiv -\sum_{i_o,\ldots,i_d} P(i_o,\ldots,i_d)\, \ell n\, P(i_o,\ldots,i_d)$

For one dimensional maps, K is just the Lyapunov exponent (see table 4.1). In higher dimensional systems, we lose information about the system because the cell in which it was previously located spreads over new cells in phase space at a rate which is determined by the

Lyapunov exponents. It is therefore plausible that the rate K at which information about the system is lost is equal to the (averaged) sum of positive Lyapunov exponents:

$$K = \int d^N x \, \rho(\underline{x}) \sum_i \lambda_i^+(\underline{x}) \qquad (4.32)$$

Here $\rho(\underline{x})$ is the invariant density of the attractor. In most cases the λ's are independent of $\underline{x}$; the integral then becomes unity and K reduces to a simple sum.

From eqn.(4.27) we have

$$e^{\lambda} = \lim_{N\to\infty} \left(\prod_{n=0}^{N-1} \left| \frac{dG}{dx_n} \right| \right)^{1/N} \qquad \text{for}$$

one dimensional map. This can be generalized to d dimensions, where we have d exponents for the different spatial directions,

$$(e^{\lambda_1}, e^{\lambda_2}, \ldots, e^{\lambda_d}) = \lim_{N\to\infty} \left[\begin{array}{c} \text{magnitude of the} \\ \text{eigen values of} \\ \prod_{n=0}^{N-1} J(x_n) \end{array} \right]^{\frac{1}{N}} \qquad (4.33)$$

where $J(x_n) = \left(\frac{\partial G_i}{\partial x_j}\right)$ is the Jacobian matrix of the map $\underline{x}_{n+1} = \underline{G}(\underline{x}_n)$.

The K entropy also measures the average time over which the system's state, displaying deterministic chaos, can be predicted. To see this consider the simple one dimensional triangular map*, in Fig.4.6, which is confined to the unit square. After n time steps, an interval ℓ increases to $L = \ell e^{\lambda n}$.

---

* The triangular or tent map is defined by

$$x_{n+1} = \frac{x_n}{\eta} \qquad 0 < x_n < \eta$$

$$x_{n+1} = \frac{(1-x_n)}{(1-\eta)} \qquad \eta < x_n < 1 \quad , \; x_n \in [0,1] \text{ (see reference 8).}$$

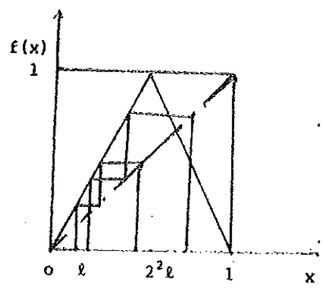

Fig. 4.6 Separation of points by iteration with $f(x) = (1 - 2|\frac{1}{2} - x|)$

If L becomes larger than 1, we can no longer locate the trajectory in [0,1] and all we can say is that the system has a probability $\rho_0(x)dx$ of being in an interval $[x, x+dx] \in [0,1]$, where $\rho_0(x)$ is the invariant density of the system. In other words, precise predictions about the state of the system are only possible for times n that are smaller than T_m:

$$\ell e^{\lambda T_m} = 1 \rightarrow T_m = \frac{1}{\lambda} \ell n\ 1/\ell \qquad (4.34)$$

Above T_m one can only make statistical predictions. Eqn.(4.34) can be generalized to higher dimensional systems by replacing λ by the K - entropy [6]:

$$T_m \propto \frac{1}{K} \ell n\ 1/\ell \qquad (4.35)$$

Let us summarize our results about the K - entropy.

- It measures the average rate at which information about the state of a dynamical system is lost with time.
- For one-dimensional maps, it is equal to the Lyapunov exponent. In higher dimensional systems K measures the average deformation of a cell in phase space and becomes equal to (the integral over phase space of) the sum of the positive Lyapunov exponents.
- It is inversely proportional to the time interval over which the state of a chaotic system can be predicted.

4.3 Characterization of an Attractor by a Measured Signal

Having observed experimentally a seemingly random signal, one wants to know what information it contains about the chaotic attractor. Partial answer to this question is contained in an infinite set of dimensions D_q introduced in sec. 4.2, which describe the inhomogenity of the attractor. It is then shown that D_2 (which yeilds a lower bound to the Hausdorff dimension, can be obtained directly from a measurement[27]. However, the time dependence of all components in phase space is still required. Fortunately, Takens' theorem states that important properties of the attractor[6,29,30], such as e.g., D_2, can be reconstructed from the measurement of a single component. It has been shown in as series of papers by Grarssberger Hentschel and Procacia that, in fact the following properties can be obtained from a single time sequence:

- D_2, i.e., a lower bound on the Hausdorff dimension ($D_2 < D$)
- d, i.e., the embedding dimension of the attractor
- The amplitude of white noise on the signal, i.e., the irregularities originating from determinstic motion on the attractor can be separated from disturbing white noise
- A lower bound on the K-entropy, i.e., it can be determined "how chaotic" the signal is

Reconstruction of an Attractor from a Time Series

It is not always possible to measure all components of the vector $\underline{X}(n)$ simultaneously. This clearly holds for an infinite-dimensional system. If we define the dimension of a system by the number of initial conditions, then the so called Mackey-Glass equation:

$$\dot{x} = \frac{ax(t-\tau)}{1+(x(t-\tau))^{10}} - bx(t) \qquad (4.36)$$

(which describes the regeneration of blood cells) obviously provides a simple example of an infinite - dimensional system, because all the $x(t)$ - values in the interval $t, t-\tau$ have to be known (as initial conditions) to solve it. How do we proceed in this or the less difficult case where we have an attractor embedded in a d-dimensional space, but measure only one component of the signal?

It has been shown by Takens that one can reconstruct certain properties of the attractor in phase space from the time series of a single component[6,29,30]. Instead of the rather cumbersome proof we present the following simplified argument. As an example, consider a two dimensional flow generated by $\dot{\underline{x}} = \underline{F}(\underline{x})$, where $\underline{x} = (x,y)$. Every point $(x(t+\tau), y(t+\tau))$ then originates uniquely from a point $(x(t), y(t))$ and the relation between both points is one-to-one because the trajectories do not corss[6] (otherwise the trajectory would not be determined by the initial conditions).

Next we construct a sequence of vectors

$$\underline{v}(t) = (x(t), \; x(t+\tau))$$
$$\underline{v}(t+\tau) = (x(t+\tau), \; x(t+2\tau)) \qquad (4.37)$$

Since the components of $\underline{v}$ are related to $(x(t), y(t))$ via the one-to-one relationship.

$$v_1(t) = x(t) \qquad (4.38a)$$
$$v_2(t) = x(t+\tau) = \int_t^{t+\tau} dt' (F_1 x(t'), y(t')) + x(t)$$
$$\approx \tau F_1(x(t), y(t)) + x(t) \qquad (4.38b)$$

with a Jacobian $|\tau \frac{\partial F_1}{\partial y}| \neq 0$ it is plausible that the information contained in the time sequence $\underline{x}(t_i)$ and $\underline{v}(t_i)$ ($t_i = i\tau$ say) is the same, and both sequences should lead to the same characteristic dimensions. A simple example for which $\underline{x}(t_i)$ and $\underline{v}(t_i)$ are indeed completely equivalent is a circle

$$\begin{aligned}\underline{x}(t_i) &= \{x(t_i),\ y(t_i)\} = \{\sin(2\pi t_i),\ \cos(2\pi t_i)\} \\ &= \{\sin(2\pi t_i),\ \sin 2\pi(t_i + \tfrac{1}{4})\} \\ &= \{x(t_i),\ x(t_i + \tfrac{1}{4})\} \\ &= \underline{v}(t_i)\end{aligned} \tag{4.39}$$

But we have to keep in mind that these arguments are only heuristic and can only be applied "cum grano salis" to situations where 'chaotic attractors' appear. What Takens actually proved is the following[6]:

"If $\dot{\underline{x}} = \underline{F}(\underline{x})$ generates a d-dimensional flow then

$$\underline{v}(t) = \{x_j(t), x_j(t+\tau), \ldots, x_j(t+(2d+1)\tau)\} \tag{4.40}$$

where $x_j(t)$ is an arbitrary component of $\underline{x}$, provides a smooth embedding for this flow, and the metric properties in both spaces (the d-dimensional $\{\underline{x}(t)\}$ and the (2d+1) - dimensional $\{\underline{v}(t)\}$) are the same in the sense that distances in $\{\underline{x}(t)\}$ and $\{\underline{v}(t)\}$ have a ratio which is uniformly bounded and bounded away from zero".

Fig.4.7 shows that plots of $\ell nC(\varepsilon)$ versus ε for the Lorenz attractor. The lower line is obtained directly from the three-dimensional time series $\{x(t_i), y(t_i), z(t_i)\}$, whereas the upper line originates from the reconstructed series $\underline{v}(t_i) = \{x(t_i), x(t_i+\tau), x(t_i+2\tau)\}$.

The slopes of both lines are the same as stated above showing that the correlation dimension is the same using both methods.

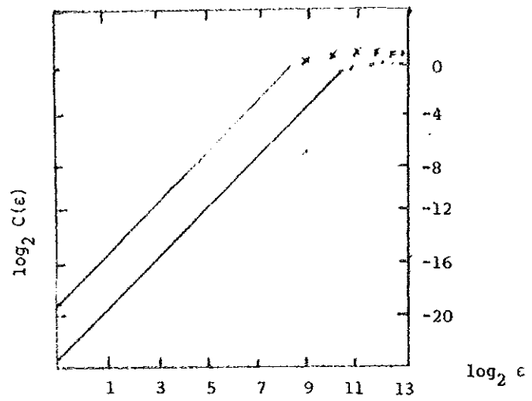

Fig. 4.7 Correlation integral for the Lorenz model on a doubly logarithimic scale, the scale of ε in arbitrary. [From reference 27].

Embedding Dimension

In Fig.4.8 the ε dependence of the correlation integral is depicted for the Mackey-Glass system. Although this system has an infinite dimension, its correlation dimension is finite and smaller than 3. It is therefore sufficient to use a single time series with three-dimensional vector $\underline{v}(t_i) = \{x(t_i), x(t_i + \tau), x(t_i + 2\tau)\}$ to determine D_2. The dimension M in $\underline{v}(t)$: $\{x(t_i),\ldots,x(t_i + (M-1)\tau\}$ above which

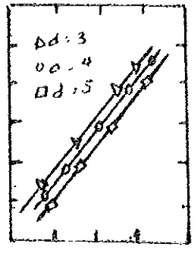

Fig. 4.8 $D_2 = 1.95 \pm 0.03$ determined from a single variable time series for the Mackey-Glass equation with parameter values $\tau = 17$, $a = 0.2$, $b = 0.1$ for different embedding dimensions M (From reference 6).

D_2 no longer changes is the (minimal) embedding dimension of the attractor. It belongs to the space with the lowest integer dimension containing the whole attractor. Lower bound for the Kolmogroff entropy. Let us recall eqn.(4.31) which relates K to a time series for a map:

$$K = -\lim_{\tau\to 0}\lim_{\varepsilon\to 0}\lim_{\alpha\to\infty}\frac{1}{d\tau}\sum_{i_1,..,i_d} P(i_1,..,i_d)\,\ell n(P(i_1,...,i_d)$$

P. Grassberger and I. Procaccia [31] defined a new quantity K_2 with the following properties:

i) $K_2 \geq 0$

ii) $K_2 \leq K$

iii) $K_2 \to \infty$ for random systems

iv) $K_2 \neq 0$ and finite for chaotic systems.

To see how this quantity comes about, consider the set of order-q Renyi entropies which are defiend as follows

$$K_q = -\lim_{\tau\to 0}\lim_{\varepsilon\to 0}\lim_{d\to\infty}\frac{1}{d\tau}\frac{1}{q-1}\ell n \sum_{i_1,..,i_d} p^q(i_1,...i_d) \qquad (4.40)$$

By writing $p^q = e^{(q-1)\ell np}$ and expanding the exponent one can reach at

$$\lim_{q\to 1^+} K_q = K$$

Furthermore, it is easy to see that $K_q > K_{q'}$ for every $q > q'$.

Of all the order -q quantities K_q, K_2 is singled out due to its ease of calculation from a time series $\{\underline{x}_i\}_{i=1}^{N}$ where $\underline{x}_i = \underline{x}(t = i\tau)$ up to an ε independent factor[31]

$$C(\varepsilon) = \lim_{N\to\infty}\frac{1}{n^2}\left[\begin{matrix}\text{number of pairs of points}\\ (n,m) \text{ with } |x_m - x_m| < \varepsilon\end{matrix}\right] \qquad (4.41)$$

On the other hand P. Grassberger and I. Procaccia showed that[28]

$$C(\varepsilon) \sim \varepsilon^{\nu} \tag{4.42}$$

and called ν the correlation dimension, $\nu \leq D$.

For any d we consider now

$$\tilde{C}_d(\varepsilon) = \lim_{N\to\infty} \frac{1}{N^2} \begin{matrix} \text{No of pairs } (n,m) \text{ with} \\ [\sum_{i=0}^{d-1} (x_{n+i}^2 - x_{m+i}^2)]^{\frac{1}{2}} \leq \varepsilon \end{matrix} \tag{4.43}$$

with $d = 2,3,\ldots$ up to a factor of unity

$$\tilde{C}_d(\varepsilon) \sim \sum_{i_1,\ldots,i_d} p^2(i_1,\ldots,i_d) \tag{4.44}$$

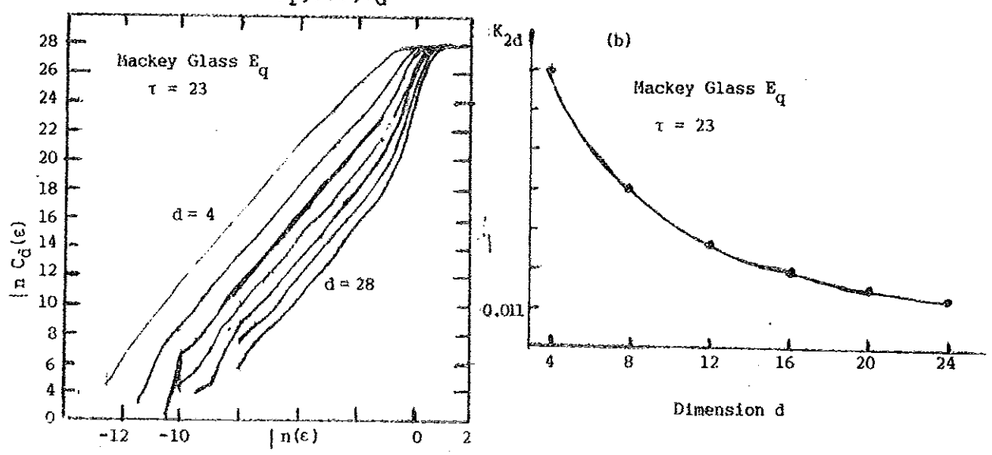

Fig. 4.8 a) Correlation integral $C_d(\varepsilon)$ for the Mackey Glass delay differential equation Vs ε. The error bars are purely statistical. Points pertainning to the same value of d are connected by lines. The values of d are d = 4 (Top curve and d = 28 bottom curve).

b) Values of $K_{2,d}$ for the Mackey Glass delay differential equation averaged over the scaling region in ε. The extrapolated ($d\to\infty$) value in K_2 = 0.008 ± 0.001 [From reference 31].

Consequently eqns.(4.40) and (4.42) leads to

$$\tilde{C}_d(\varepsilon) \underset{\substack{d\to\infty \\ \varepsilon\to 0}}{\sim} \varepsilon^{\nu} e^{-K_2 \tau d} \tag{4.45}$$

In practice we do not need to follow the evolution of all the degrees of freedom. Generically, the whole trajectory can be reconstructed from d measurements ($d \geq N$) of any single coordinate. Taking any coordinate and denoting it by x, we consider then

$$\tilde{C}_d(\varepsilon) = \lim_{N\to\infty} \frac{1}{N^2} \left[\begin{array}{l} \text{No of pairs } (n,m) \text{ with} \\ [\sum_{i=1}^{d} (\underline{x}^2_{n+i} - \underline{x}^2_{m+i})]^{\frac{1}{2}} < \varepsilon \end{array} \right] \qquad (4.46)$$

and expect it to give the same estimate $C_d(\varepsilon) \sim e^{\nu} d^{-K_2 d\tau}$

Before closing this section let us briefly review the Kaplan-Yorke conjecture. The question here is, what is the connection between dynamical properties measured by $D'_q s$?

The topological dimension of the attractor is directly related to the number of non-negative characteristic exponents[5,6,31]

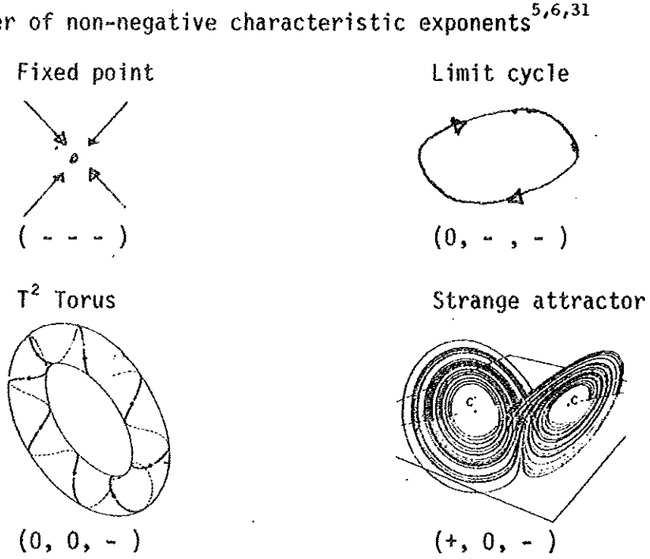

Fig.4.9 Signs of Lyapunov, exponents of different types of attractor in 3-D phase space (From reference 5).

Relationship between dimension of chaotic attractors and Lyapunov exponents.

Let $\lambda_1, \lambda_2, \ldots, \lambda_N$ be the Lyapunov numbers of the map ordered so that $\lambda_1 > \lambda_2 > \ldots > \lambda_N$. Then Kaplan and Yorke conjecture[32,35] that

$$D_o = j + \frac{\ell n\ (\lambda_1 \lambda_2, \ldots, \lambda_j)}{\ell n\ (1/\lambda_{j+1})} \tag{4.47}$$

where j is the largest number for which $\lambda_1 \lambda_2, \ldots \lambda_j > 1$, and

$$\lambda_i = \lim_{q \to \infty} \left[\begin{array}{l} \text{magnitude of the eigenvalue} \\ \text{of } J(\underline{x}_q)\ J(\underline{x}_{q-1}) \ldots J(\underline{x}_2)\ J(\underline{x}_1^1) \end{array} \right]^{\frac{1}{q}},$$

$x_1, x_2, \ldots, x_d$ a sequence generated by the map under discussion (of the type $x_{j+1} = f(x_j)$).

In order to apply eqn.(4.47) to the case of ordinary differential equations Kaplan and Yorke introduced Lyapunov exponents $h_1, h_2, \ldots, h_N$, where N is the dimension of the system. Viewing the ordinary differential equation as generating a map advancing $\underline{x}$ forward by some constant increment in time τ, one identify[32]

$$\lambda_i = e^{h_i \tau} \tag{4.48}$$

inserting the λ_is into (4.47) we obtain:

$$D_o = j + \sum_{i=1}^{j} h_i / |h_{j+1}| \tag{4.49}$$

Russel et al[32] tested the validity of (4.47) for three different two dimensional maps (Henon map, Kaplan and Yorke map and Zaslaviskii map) the result seems valid only for uniform attractors, and its range of applicability is still an active field of research.

4.4. Experimental Illustration of Chaotic Attractors

Our first example is from chemistry: the B-Z* reaction, the one we have seen in chapter 2. The variable measured is the concentration of bromide ions in the reactor. Recordings of the time series $X(t_i)$ containing several tens of thousands of points have been made for a fixed value of the reactant flux (the control parameter μ). Phase portrait are obtained by the method of time delays (see section 4.4) which gives a representation of the attractor in a 3-D phase space with coordinates $x(t_i)$, $x(t_i+\tau)$, $x(t_i+2\tau)$.

For certain values of the reactant flux, the reaction is periodic and the phase portrait is then a limit cycle, representable in a space of two dimensions. The situation changes radically for other flux values where chaotic regimes can be found, as the phase portrait projection of Fig.4.10 testifies.

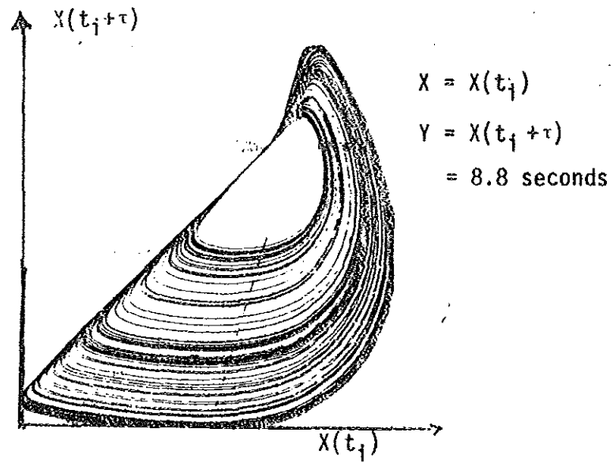

Fig. 4.10 Chaotic region of the B-Z reaction (From reference 5).

---

* Belousov-Zhabotinsky

Apart from its aesthetic interest, this projection tells us little about the dynamical state of the system. It would be risky to conclude on the sole evidence of Fig.4.10 that we have a strange attractor. The same uncertainity in interpretation could exist even if we represented the attractor in a 3-D phase space. A decisive step is taken, however, when we make a Poincare section through a 3-D representation of the attractor, the third coordinate being $X(t_i+2\tau)$ The plane of section is perpendicular to the plane of Fig.(4.10) on which it is represented by dashed lines.

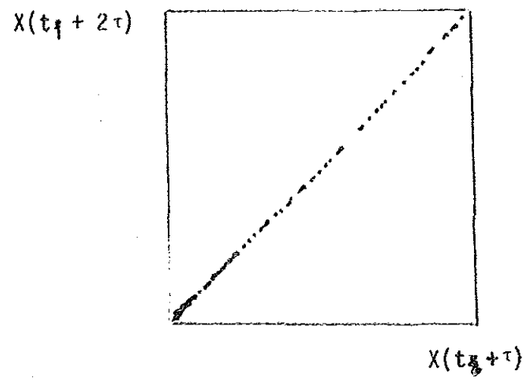

Fig. 4.11 Poincare Section

This is a section through the trajectories in the $X(t)$, $X(t+\tau)$, $X(t + 2\tau)$ space of which Fig. 4.10 is a projection. The plane of section is perpendicular to that of Fig.4.10, where their intersection is marked by a dashed line. (From reference 5).

The determinstic nature of the chaotic attractor can be indisputably confirmed by the first return map which can be constructed from the Poincare map when the dissipation rate is great. By graphing the ordinate X_{k+1} of a point on Fig.4.11 as a function of the ordinate X_k of its antecedent, we see from Fig.4.12 that all of the points are located on a well-defined curve.

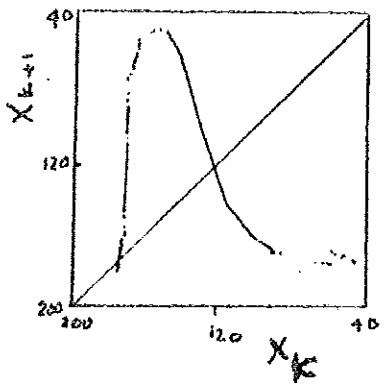

Fig. 4.12 Return map. Minimum in bromide ion electrode potential vs the value at the previous minimum. (From reference 33).

A mathematical representation of the above curve was developed by filling the data as follows[33] :

$$Y = \begin{cases} 175 - 4.42[1.44 - (x-172)]^{1/3}\, e^{0.0126x} & , \; x \geq 172 \\ 175 - 4.42[1.44 + (x-172)]^{1/3}\, e^{0.0126x} & , \; 172 > x \geq 150 \\ 175 - 182(175 - x)^{2.04}\, e^{0.0918x} & , \; 150 > x \geq 60 \\ 191 - 0.375x & , \; x < 60 \end{cases}$$

where for convenience we write

$$Y = Br(min)_{n+1} \quad \text{and} \quad X = Br(min)_n$$

Hudson and Mankin found, that the largest Lyapunov exponent for the above return map to be

$$\bar{\lambda} = 0.62$$

The fact that $\bar{\lambda} > 0$ implies that the trajectories diverge and that the behavior of the system is chaotic.

Another example comes from optics where we quickly review the results of N.B. Abraham et al[34] where D_2 and K_2 of output intensity time sequences from Xe - He ring laser were calculated. Their analysis shows that the Caser's dynamics is characterized by an attractor of relatively low dimensionality. (For experimental set-up see reference 34).

D_2 and K_2 were calculated for each data set, which were taken for different cavity detunings (or cavity length), using the technique developed by Grassberger and Procaccia[31]:

For each set of N numbers,

$$\{ x_i \mid i = 1,2,\ldots, N \}$$

where $X_j = x(j\tau)$, j an integer and τ (= 1ns in this case) the time interval between measurements M-dimensional time-delay vectors were formed

$$\underline{Y}_k = (X_k, X_{k+1},\ldots, X_{k+d-1})$$

Using these vectors

$$C_M(\varepsilon) = \frac{1}{N_M} \sum_{j=k}^{} \theta(\varepsilon - |\underline{Y}_k - Y_j|)$$ where N_M is the

pairs of M-dimensional vectors used in the sum. For sufficiently small ε's and large embedding dimensions, M, the correlation sum scales as,

$$C_M(\varepsilon) \sim e^{D_2} \; e^{-\tau M K_2}$$

$$C_M(\varepsilon) \equiv C_M(\varepsilon, M, D_2, K_2)$$

$$\Longrightarrow \quad D_2 = \lim_{\varepsilon \to 0} \lim_{M \to \infty} \frac{d[\ell n\, C_M(\varepsilon)]}{d[\ell n\, \varepsilon]}$$

$$\text{and} \quad K_2 = \lim_{\varepsilon \to 0} \lim_{M \to \infty} \ell n[C_M(\varepsilon) \mid C_{M+1}(\varepsilon)|]$$

In practice, ε is limited from below by noise and M is eventually limited from above by the size of the data set, although a more stringent limit on M is usually set by constraints on computing time.

For the purposes of discriminating between chaotic signals and random noise, the important properties of D_2 are that it should be 1 for a periodic signal, 2 for signals characterized by two incommensurate frequencies, finite and greater than two for chaotic signals and infinite for random signals. For K_2 see sec. 4.3-1.

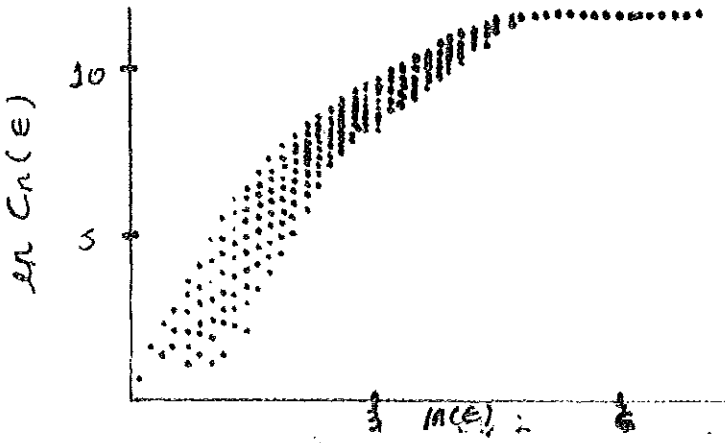

Fig.4.13 $\ln C_n(\varepsilon)$ vs $\ln \varepsilon$ for a chaotic laser out-put. Embedding dimensions 10-20. (From reference 34).

The graph of slope vs $C_M(\varepsilon)$ also found to show a plateau at 2.6 ± 10% meaning that the dimension of the system is fractal and $2 < d < 3$.

Our last experimental illustration, where the methods of nonlinear mechanics has got applications, comes from medicine: chaotic attractors in human cortex.

The electrical activity of the brain can be recorded by electrocephographic techniques (EEG) and is used in medical diagnosis. This

electrical information may be analyzed in various ways in order to obtain some clues regarding the structure and function of the brain. The developments made on nonlinear dynamics since 1971 have provided new methods which are particularly interesting for the analysis of data obtained from complex systems such as the EEG.

In the framework of this nonlinear dynamic theory, one may find answers to the following questions: does the system under consideration obey a deterministic dynamics, with reducible phase relationships, or does the great variability seen in a given complex system reflect random, therefore irreducible, process? For instance, Fig. 4.14c, shows the EEG record during the time of epileptic petitmal seisure. Although at first sight the phenomenon appears periodic in time, a closer scrutiny shows pseudoperiods with obvious variabilities[40]. It is interesting to know if this variability is due to random noise or is determined by a determinstic dynamics.

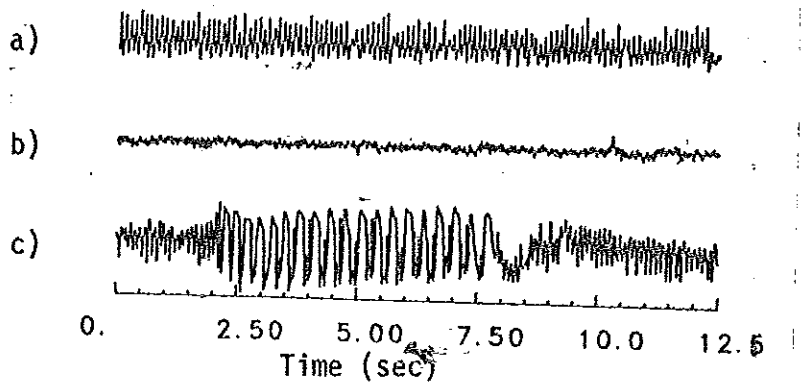

Fig. 4.14 EEG of human brain activity from three different stages.

a) alpha rythm (eyes closed)

b) beta rythm (eyes open)

c) petit-mal (epilepsy). [From reference 40].

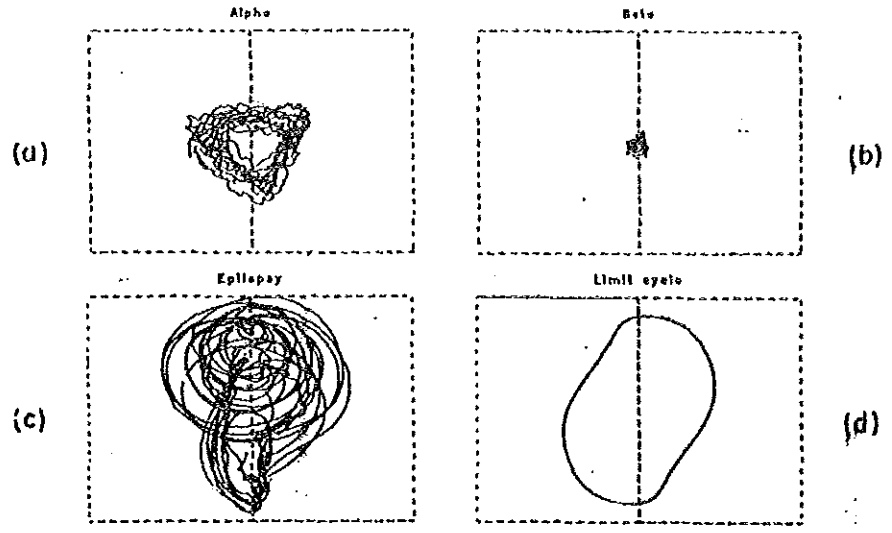

Fig. 4.15 Phase portraits of brain waves constructed from the EEG of Fig.4.14.

a) alpha rhythm (3 sec., τ = 33 m.sec)

b) beta rhythm (3 sec., τ = 33 m.sec)

c) petit-mal (6 sec., τ = 8 m.sec)

These are the two dimensional projections of the three dimensional phase space

d) a limit cycle. [From reference 40].

From these phase portrait we see that, alpha and beta wave trajectories form a far more diffuse object than those of epilepsy. There fore, this low coherence may indicate deterministic dynamics of relatively large number of variables or a very "noisy" brain activity.

Applying, the Procedure of sec. (4.3).

A.Babloyantz and A. Destexhe obtained the correlation dimension for α-waves. The value is $\nu_\alpha = 6.10 \pm 0.5$.

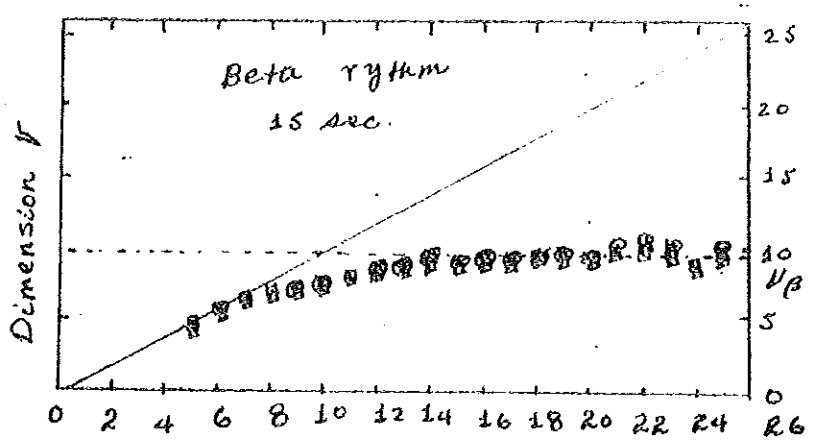

Fig. 4.16 Saturation curve obtained from beta waves. 15 sec. EEG are used with 240 Hz and with four different delays: $10\Delta t$ (x), $20\Delta t$ ( ), $30\Delta t$ (Δ) and $40\Delta t$ (0). [From reference 40].

Fig.4.15 shows Babloyantz and Destexhe atempt at the characterization of beta waves. Saturation is obtained for $\nu_\beta = 9.7 \pm 0.7$. But is the Grassberger procaccia (method) algorithm still holds for such a high dimension? This remains to be seen (studied).

From these results it is seen that brain activity with open eyes seems to obey either random processes or is described by an attractor of very high dimension. When eyes are closed and the subject drifts toward sleep, then brain activity jumps from one attractor to the next. For a normal brain, the lowest dimensionality is seen in the sleep stage 4.

CONCLUSION

The Methods of non-linear dynamics, reviewed in this work, have far reaching applications in a wide variety of fields.

Dissipative systmes can be well described by their attractors. Those systems which exhibit chaotic behavior have chaotic attractors and the dimension of these attractors are fractal (non-integer). Therefore, some knowledge of fractal geometry is essential.

Chaotic attractors can be characterized by their metric and dynamical properties, notably, by their dimensions and Kolmogrov entropy.

The methods of non-linear dynamics are specailly valuable for the analysis of experimental data obtained from a single variable time series. From this series, one can construct the whole trajectory in an artificial phase space. Calculating the correlation dimension of this reconstructed attractor, we obtain valuable information about the dimensionality of our system. This will be of help in modelling the system under investigation.

REFERENCES

1. TH. Brocker and K. Janicn, Introduction to Differential Topology, Cambridge University Press (1982).

2. E. Ott, Rev. Mod. Phys., 53 , 655 (1981).

3. J.P. Eckmann, Rev. Mod. Phys. 53, 643 (1981).

4. J.J. Stoker Nonlinear Vibrations, Interscience Publishers, Inc., New York, 2 (1950).

5. Y. Pomaeu, P. Berge and C. Vidal, Order within Chaos, by Hermann, Paris, France (1984).

6. H.G. Schuster, Deterministic Chaos, an Introduction Physik-Verlag, Weinheim (1984).

7. Masaya Yamaguti and Masayoshi Hata, Lecture Notes in Num. App.Anal. 5, 361 (1982).

8. H. Atmanspacher, H. Scheingraber, and W. Vogos, Phys. Rev. 37A , 1314 (1988), R. Baddi, K. Heinzelmann, P.F. Meir and A.Politi, ibid, page 1323.

9. M.J. Feigenbaum, Loss Almos Science, 1, 4(1980).

10. P. Civitanovic, Universality in Chaos, Adam Hilger Limited (1984).

11. E.N. Lorenz, J. Atoms. Sci., 20, 130 (1963).

12. J.B. Maclaughlin and P.C. Martin, Phys. Rev. 12A , 186 (1975).

13. B. Saltzman, J. Atmos. Sci. 19, 329 (1962).

14. R. Gilmore, Catastrophe Theory for Scientists and Engineers, by Jhon Wiley and Sons, Inc., (1981).

15. D. Ruelle, Math Intelligencer, 2, 126 (1980).

16. R. H.G. Helleman, Fundamental Problems in Statistical Mechanics, 5, 165 (1980).

17. M.J. Feigenbaum, M.H. Jensen, I. Procaccia Phys. Rev. Lett. 57, 1503 (1986).

18. M. Henon, Comm. Math. Phys. 50, 69 (1976).

19. R.M. May, Nature 261, 459 (1976).

20. A.L. Goldberger, Springer Series in Syn. 36, 118 Springer-Verlog Berlin Heidelberg (1987).

21. J.P. Keener Ibid page 134.

22. Thomas C. Halsey et al, Phys. Rev. 33A, 1140 (1986).

23. M. Barnsley, Fractals Everywhere, by Acadamic Press, Inc. (1988).

24. B. Rohricht et al, Springer series in Syn. 37, 275, Springer-Verlo Berlin Heidelberg (1987).

25. C. Grebogi, E. Ott, and J.A. Yorke Phys. Rev., 37A, 1711 (1988).

26. B. Dorizzi, et al, PHys. Rev., 35A 328 (1987).

27. P. Grassberger and I. Procaccia Phys. Rev. Lett. 50, 346 (1983).

28. K. Pawelzik, and H.G. Schuster Phys. Rev. 35A, 481 (1987).

29. A.I. Mees, P.E. Rapp, and L.S. Jennings, Phys. Rev. 36A, 340 (1987

30. A.M. Albano et al, Phys. Rev. 38A, 3017 (1988).

31. P. Grassberger and I. Procaccia Phys. Rev. 28A, 2591 (1983).

32. David A. Russel, James D. Hansen and E. Ott, Phys. Rev. Lett, 45, 1175 (1980).

33. J.L. Hudson and J.C. Mankin, J. Chem. Phys. 74, 6171 (1981).

34. N.B. Abraham et al, Perspectives in Nonlinear Dynamics, Edited by Shlesinger, R. Cawley, A.W., W. Zachary, World Scientific Publishing Co. Pvt. Ltd., 214 (1986).

35. N.H. Packard, J.P. Crutchfield, J.D. Farmer and R.S. Shaw, Phys. Lett. 45, 712 (1980).

36. J. Guckenheimer reference 34 page 279.

37. Alen C. Newell Ibid page 38.

38. YU.L. Klimontovich-Springer Series in Syn., 31,32 Springer-Verlog Berlin Heidelberg (1985).

39. Jack K. Hale, reference 34 page 281.

40. A Babloyantz and A. Destexhe, reference 20 page 48.